environmental microbiology

Environmental Microbiology (2022) **24**(4), 2059–2077 doi:10.1111/1462-2920.15958

Some like it cold: the cellular organization and physiological limits of cold-tolerant nitrite-oxidizing *Nitrotoga*

Sabine Keuter,[1†] **Hanna Koch**,[2†] **Katharina Sass**,[1] **Simone Wegen**,[1] **Natuschka Lee**,[3,4] **Sebastian Lücker**[2] **and Eva Spieck**[1*]

[1]*Department of Microbiology and Biotechnology, University of Hamburg, Hamburg, Germany.*

[2]*Department of Microbiology, RIBES, Radboud University, Nijmegen, The Netherlands.*

[3]*Department of Ecology and Environmental Science and Research Infrastructure Fluorescence in situ Hybridization (FISH), Chemical Biological Centre, Umeå University, Umeå, Sweden.*

[4]*Department of Microbiology, Technical University of Munich, Freising, Germany.*

Summary

Chemolithoautotrophic production of nitrate is accomplished by the polyphyletic functional group of nitrite-oxidizing bacteria (NOB). A widely distributed and important NOB clade in nitrogen removal processes at low temperatures is *Nitrotoga*, which however remains understudied due to the scarcity of cultivated representatives. Here, we present physiological, ultrastructural and genomic features of *Nitrotoga* strains from various habitats, including the first marine species enriched from an aquaculture system. Immunocytochemical analyses localized the nitrite-oxidizing enzyme machinery in the wide irregularly shaped periplasm, apparently without contact to the cytoplasmic membrane, confirming previous genomic data suggesting a soluble nature. Interestingly, in two strains we also observed multicellular complexes with a shared periplasmic space, which seem to form through incomplete cell division and might enhance fitness or survival. Physiological tests revealed differing tolerance limits towards dissolved inorganic nitrogen concentrations and confirmed the generally psychrotolerant nature of the genus. Moreover, comparative analysis of 15 *Nitrotoga* genomes showed, e.g. a unique gene repertoire of the marine strain that could be advantageous in its natural habitat and confirmed the lack of genes for assimilatory nitrite reduction in a strain found to require ammonium for growth. Overall, these novel insights largely broaden our knowledge of *Nitrotoga* and elucidate the metabolic variability, physiological limits and thus potential ecological roles of this group of nitrite oxidizers.

Received 10 December, 2021; revised 18 February, 2022; accepted 24 February, 2022. *For correspondence. E-mail eva.spieck@uni-hamburg.de; Tel. +49 40 42816 424; Fax +49 40 42816 459. †Keuter and Koch should be considered joint first authors.

Introduction

Nitrification, the oxidation of ammonia to nitrite (ammonia oxidation) and further to nitrate (nitrite oxidation) is an essential microbial process in the global biogeochemical nitrogen (N) cycle. It is the only known biological process producing nitrate and thus provides N in its most oxidized state (+V), which is an important electron acceptor under anoxic conditions, but also can be utilized as N source by many organisms. Consistent with their ecological importance, nitrifying microorganisms are ubiquitous and encompass a large phylogenetic diversity. Chemolithoautotrophic nitrite oxidation has apparently evolved more than once in different bacterial lineages (Daims *et al*., 2016) and was hitherto described in 10 genera of the four bacterial phyla Proteobacteria (with members in the three classes Alpha-, Beta- and Gammaproteobacteria), Nitrospirae, Nitropinae and Chloroflexi. Interestingly, several new genera have been discovered during recent years, such as *Ca*. Nitronauta and *Ca*. Nitrohelix within the Nitrospinae (Mueller *et al*., 2021), *Ca*. Nitrocaldera and *Ca*. Nitrotheca within the Chloroflexi (Spieck *et al*., 2020b), and further lineages were identified in metagenomic datasets (e.g. *Ca*. Nitromaritima; Ngugi *et al*., 2016). While the ubiquitous *Nitrospira* is deemed the most diverse genus with several sublineages occupying different ecological niches and numerous habitats (Pester *et al*., 2014; Daims *et al*., 2016), other NOB groups seem to be more restricted to certain ecosystems. *Nitrospina* and *Nitrococcus* for instance are found exclusively in marine environments, while sequences of Chloroflexi-affiliated NOB like *Nitrolancea* have to date

predominantly been obtained from high-temperature systems, partly also at elevated ammonium concentrations (Sorokin *et al*., 2012; Spieck *et al*., 2020a). In comparison, the betaproteobacterial genus *Nitrotoga* occurs in a wider range of natural as well as man-made ecosystems, similar to *Nitrobacter* (Vanparys *et al*., 2007; Boddicker and Mosier, 2018). For example, based on 16S rRNA gene surveys as well as culture-dependent studies, *Nitrotoga* occurs 800 m below ice in Antarctica, in periglacial soil at 5400 m altitude in the Andes, in rivers as well as in wastewater treatment plants (WWTPs; Schmidt *et al*., 2009; Christner *et al*., 2014; Fan *et al*., 2016; Boddicker and Mosier, 2018; Spieck *et al*., 2021). While in most studies on wastewater treatment systems *Nitrospira* has been identified as the dominant NOB group, *Nitrotoga* was found to be dominating in certain WWTPs, suggesting that they can play a primary role in N removal (Lücker *et al*., 2015; Saunders *et al*., 2016).

Regarding energy conservation and carbon fixation, NOB can generally be grouped based on the localization of their key enzyme for nitrite oxidation, the nitrite oxidoreductase (NXR) complex. One group possesses an NXR facing the cytoplasm and uses the Calvin–Benson–Bassham (CBB) cycle (*Nitrobacter*, *Nitrococcus*, *Nitrolancea*) (Starkenburg *et al*., 2008; Sorokin *et al*., 2012; Füssel *et al*., 2017), while the other has a periplasmic NXR and uses the reverse tricarboxylic acid (TCA) cycle for carbon fixation (*Nitrospira*, *Nitrospina*) (Lücker *et al*., 2010, 2013; Mueller *et al*., 2021). *Nitrotoga*, however, deviates from these major groups, as genomic predictions suggested that it uses the CBB cycle but has a periplasmic NXR (e.g. Kitzinger *et al*., 2018). However, this predicted cellular localization of the NXR awaits experimental confirmation.

The orientation of the NXR complex could affect the affinity and sensitivity of an NOB to nitrite and is therefore an important niche-defining factor (Daims *et al*., 2011; Nowka *et al*., 2015a). A periplasmatic NXR, when organized in such a way that its active centre is in close vicinity to the periplasmic face of the cytoplasmic membrane, is more energy efficient since the protons generated during nitrite oxidation might directly contribute to the proton motive force (Lücker *et al*., 2010). Moreover, periplasmic nitrite oxidation is not dependent on nitrite transport into the cells, thus avoiding transport limitations. Compatibly, NOB clades with a periplasmic NXR, such as *Nitrospira* and *Nitrospina*, have high nitrite affinities and consequently inhabit niches with low nitrite concentrations (Nowka *et al*., 2015a).

In addition to nitrite availability, pH and temperature define ecological niches of NOB, and these environmental factors were pivotal in the enrichment efforts of several *Nitrotoga* strains (Alawi *et al*., 2007; Hüpeden *et al*., 2016). In competition with *Nitrospira*, *Nitrotoga* was flourishing when either temperature (Alawi *et al*., 2007; Karkman *et al*., 2011; Achberger *et al*., 2016; Saunders *et al*., 2016; Liu *et al*., 2017; Wegen *et al*., 2019), pH (Hüpeden *et al*., 2016; Vieira *et al*., 2019), or both were low (Ma *et al*., 2017). However, some *Nitrotoga* were found to proliferate also in mesophilic ecosystems and culture conditions (Kitzinger *et al*., 2018; Zheng *et al*., 2020; Lantz *et al*., 2021), challenging the paradigm of cold-adaptation of *Nitrotoga*.

The first *Nitrotoga* strain was obtained from Siberian permafrost soil in 2007, but until now only few enrichments and isolates exist (Alawi *et al*., 2007; Hüpeden *et al*., 2016; Boddicker and Mosier, 2018; Kitzinger *et al*., 2018; Wegen *et al*., 2019; Ishii *et al*., 2020). The scarcity of cultivated strains is due to the tedious nature of *Nitrotoga* in culture, and so physiological and morphological properties of this NOB group are still understudied.

To fill these knowledge gaps, we present such features of seven cultured *Nitrotoga* strains. In addition, the genomes of five species were analysed: two from permafrost soil including *Nitrotoga arctica* (Alawi *et al*., 2007), strain HW29 from a freshwater recirculating aquaculture system (RAS) (Hüpeden *et al*., 2016), strain BS from activated sludge (Alawi *et al*., 2009; Wegen *et al*., 2019) and a novel strain enriched from marine aquaculture that was detected in a previous study (Keuter *et al*., 2017). This first marine *Nitrotoga* was studied in detail, and its physiological characteristics are compared with those of the other strains. The goal of the present study is to deepen our understanding of *Nitrotoga* physiology, their genomic repertoire as well as the (immunocytochemical) properties of the key enzyme NXR, and thus to identify key features that facilitate the ecological success of this intriguing NOB. Moreover, some *Nitrotoga* strains were found to form cell clusters sharing the same periplasm, similar to cable bacteria or certain cyanobacteria. While the exact physiological function of these structures remains unclear, a shared periplasm might be of advantage under certain conditions for *Nitrotoga* as shown for other bacteria. For convenience and in anticipation that *Nitrotoga* will be accepted as genus name (Oren *et al*., 2020), we are omitting the prefix '*Candidatus*' in the present work.

Results and discussion

Enrichment of novel Nitrotoga *strains*

In this study, we investigated the physiology and morphology of seven *Nitrotoga* strains and analysed the genomes of five of them. Four strains (*N. arctica*, BS, HW29, HAM-1) have been described in previous studies (Alawi *et al*., 2007, 2009; Hüpeden *et al*., 2016; Wegen *et al*., 2019), whereas three novel strains (1052, Äspö terrace, *N. ponti*) were enriched and cultivated in this study.

Like *N. arctica*, the novel strains showed the typical irregularly shaped wide periplasmic space. Cells formed short or curved rods or were coccoid, and formed loose cell aggregates (Fig. 1A–D, Supplementary Fig. S1).

Strain 1052 (Fig. 1B and C) originates from permafrost soil continuously frozen since the middle to late Holocene (>3000 years ago). Lipid biomarker analyses with samples from this depth have shown the presence of living archaea and bacteria (Bischoff *et al*., 2013), but whether strain 1052 has been active throughout time is not known. Most probably, however, it is a living fossil and merely survived in a frozen state (Abramov *et al*., 2021), and hence was adapted to the warmer climate of the Middle to Late Holocene (Wetterich *et al*., 2008). This is the second *Nitrotoga* strain enriched from permafrost soil in Siberia. However, the permafrost soil samples containing *N. arctica* were taken from the active surface layer, which is subject to an extreme temperature regime (−48°C in winter and max. 18°C in summer). Thus, the two permafrost strains might be adapted to very different environmental conditions. Strain 1052 was enriched in mineral medium at different temperatures ranging from 17°C to 22°C and further purified by optical tweezing followed by a dilution series up to the step 10^{-7}. According to 16S rRNA gene amplicon sequencing it was enriched to 75% relative abundance (Supplementary Fig. S2).

The marine *Nitrotoga* cultures M3 and M5 (Fig. 1D, Supplementary Fig. S1) were enriched from carrier elements from bioreactors connected to a marine RAS that was run with North Sea water (Büsum, Germany). The cultures were incubated for 4 years at 10°C, routinely replenished with nitrite, transferred three times to fresh 70% seawater medium, and finally shifted to 22°C. In both cultures the same species was enriched, which was termed *Nitrotoga ponti* (pon'ti. L. gen. n. ponti of the sea) with respect to its origin, the North Sea. Strains M3 and M5 were enriched to about 58% and 44% respectively, according to 16S rRNA gene amplicon libraries (Supplementary Fig. S2).

Strain 'Äspö terrace' (Fig. 1A) was obtained from a biofilm sample from the Äspö Hard Rock Laboratory in Sweden and was cultivated at 10°C and initially at pH 6. Although at this pH only slow growth was observed, these conditions were inhibiting the initially coexisting *Nitrospira* population. Thus, growth of *Nitrospira* ceased to the point that they were no longer detected by PCR.

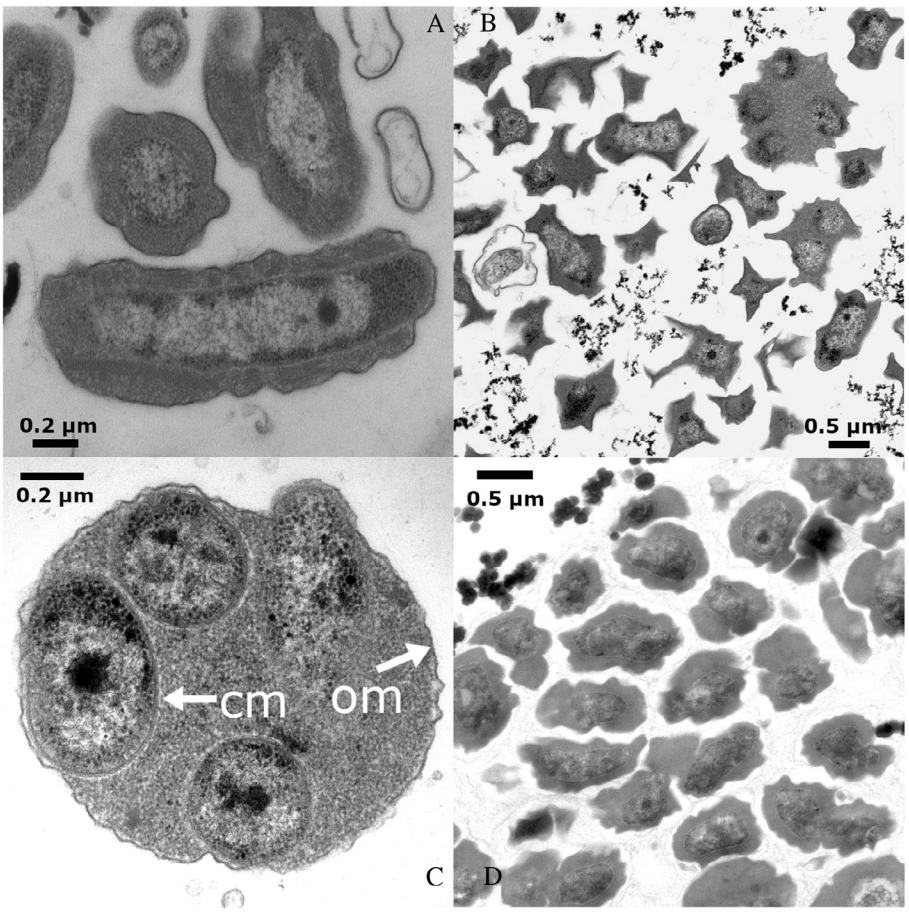

Fig. 1. Transmission electron micrographs of *Nitrotoga* cultures in ultrathin sections.
(A) Äspö terrace cells, (B) strain 1052 in overview and (C) as close-up on a complex of four cells sharing their periplasm, (D) cells of culture M5 (*N. ponti*). Cm, cytoplasmic membrane; om, outer membrane.

Subsequently, pH was set to 7.4 and *Nitrotoga* growth rate increased.

Multicellular organization in Nitrotoga

In ultrathin sections of strains 1052 and *N. arctica* potential multicellular complexes were observed containing up to six individual cells (Fig. 1B and C). These complexes are enclosed by a common outer membrane and the cells thus share the periplasmic space, which is probably a consequence of incomplete cell division. It is intriguing to note here that also single cells of the described *Nitrotoga* strains display an extremely wide periplasm, and that this compartment is filled with electron-dense particles predicted to represent NXR, the key enzyme of nitrite oxidation (see chapter *Nitrite oxidation*). A shared periplasm is known from filamentous bacteria like Actinobacteria, cyanobacteria or cable bacteria (Mariscal *et al*., 2007; Lyons and Kolter, 2015; Cornelissen *et al*., 2018). Such enlarged protected units may be formed as a survival strategy in changing and unpredictable environments and might offer advantages like improved acquisition of resources in comparison to individual, separated cells (Tecon and Leveau, 2016). Furthermore, multicellularity and its consequential size accretion can function as resistance mechanism against predation (Justice *et al*., 2008). On the other hand, a collective energy conservation by sharing their nitrite-oxidizing machinery would be comparable to other cooperative behaviour like, for instance, excretion of exoenzymes (Berleman and Kirby, 2009). Yet, there is no plausible apparent benefit resulting for *Nitrotoga* from this kind of cooperative behaviour with its own clones. This is a fascinating avenue for future research and it remains to be investigated what factors initiate incomplete cell division of some *Nitrotoga* cells resulting in this shared periplasmic space and if nutrient availability or tolerance against environmental stress factors are potential triggers, as described for multicellular system of other bacteria (Yu *et al*., 2016).

Comparison of physiological limits in Nitrotoga

Comparing published and new physiological data from this study (Table 1), all *Nitrotoga* strains seem relatively tolerant towards high concentrations of dissolved inorganic nitrogen species. Ammonium was tolerated up to concentrations of 25 (strain 1052) to 40 mM (*N. ponti*, *N. arctica*, strain HW29). While it is probably the free ammonia (FA) that becomes toxic for the bacteria at certain levels (Philips *et al*., 2002), several reactor experiments have shown that *Nitrotoga* can dominate over other NOB at even extremely high levels of FA (see Spieck *et al*., 2021 and therein).

Similar to *Nitrospira*, also the tolerance thresholds against elevated nitrite concentrations differ between *Nitrotoga* strains (Table 1, Supplementary Fig. S3), but this range starts at a higher level than for *Nitrospira* (Off *et al*., 2010; Nowka *et al*., 2015b). The permafrost strains 1052 and *N. arctica* were inhibited at the lower end of the range, namely, by >4 mM nitrite, similar to strain BS. Contrastingly, *N. ponti* was active in nitrite concentrations up to 20 mM (highest concentration tested), and thus has a substrate tolerance comparable to *N. fabula* or AMP1 (Table 1). In comparison, of all *Nitrospira* strains published, only *N. defluvii* and two marine strains tolerate such high nitrite concentrations (Keuter *et al*., 2011; Haaijer *et al*., 2013; Nowka *et al*., 2015b). The high tolerance levels of the *Nitrotoga* strains are congruent with the K_M values for nitrite determined for the strains *N. arctica* (58 μM), HAM-1 (43 μM), HW29 (60 μM), *N. fabula* (89 μM) and AM1 (25 μM), which are lower than those of *Nitrobacter* but higher than of most *Nitrospira* (Nowka *et al*., 2015a; Ishii *et al*., 2017; Kitzinger *et al*., 2018; Wegen *et al*., 2019).

Like other NOB, nitrate in concentrations up to 4 mM is not impairing nitrite oxidation of any strain tested. Strains HW29, 1052 and *N. arctica* showed reduced activity above 10 mM, and strain 1052 was even completely inhibited by 15 mM nitrate (Supplementary Table S1). *Nitrotoga ponti* showed only slightly reduced nitrite oxidation rates in the presence of 20 mM nitrate (the highest concentration tested) and therefore appears to have a similar tolerance level against nitrate as *N. fabula* and strain BS (Kitzinger *et al*., 2018; Wegen *et al*., 2019).

With respect to temperatures, the known *Nitrotoga* strains, except *N. fabula*, cover the cold spectrum in nitrite oxidation. *Nitrotoga* are the only cultured NOB that consistently show growth at 4°C and often are the dominating NOB in polar ecosystems, or also WWTPs running at low temperatures (Alawi *et al*., 2007; Christner *et al*., 2014; Lücker *et al*., 2015; Liu *et al*., 2021; Spieck *et al*., 2021). It should be noted that also *Nitrospira* have been detected in cold (e.g. permafrost) soil samples, but to date, no *Nitrospira* or other NOB with such low-temperature optima have been successfully cultivated (Sanders *et al*., 2019).

Nitrotoga arctica has its temperature optimum at 17°C and is therefore psychrotolerant, not psychrophilic (Alawi *et al*., 2007; Moyer *et al*., 2017). Interestingly, even after several years of incubation at 10°C we did not observe an adaptation to a lower temperature optimum (Fig. 2A). Similarly, also strains BS and AM-1 grew best at 17°C (Ishii *et al*., 2017; Wegen *et al*., 2019). Strain 1052, which is the second *Nitrotoga* enriched from permafrost, and the marine strain showed optimal growth at 22°C (Fig. 2A). These slightly higher temperature optima are shared with the aquaculture strain HW29 and AMP-1

Table 1. Overview of tolerances towards dissolved inorganic nitrogen species and temperature optima of the strains tested in this study in comparison with data published previously.

Strain	Origin	Reference	Ammonium	Nitrite	Nitrate	Opt. temperature
N. ponti	Biofilter marine RAS	This study	min. 40 mM	min. 20 mM	min. 20 mM	22°C
1052	Permafrost soil, core	This study	25 mM	4 mM	10 mM	22°C
N. arctica 6680	Permafrost soil, active layer	This study	min. 40 mM	4 mM	20 mM	13°C–19°C
		Alawi *et al*. (2007)		1.2 mM		10°C–17°C
BS	Activated sludge	Wegen *et al*. (2019)	30 mM	4 mM	min. 20 mM	17°C
HW29	Biofilter freshwater RAS	This study	min. 40 mM		15 mM	
		Hüpeden *et al*. (2016)		8 mM		22°C
AM-1	Eelgrass sediment	Ishii *et al*. (2017)	30 mM			16°C
AMP1		Ishii *et al*. (2020)		20 mM		20°C–23°C
N. fabula	WWTP	Kitzinger *et al*. (2018)		min. 30 mM	25 mM	24°C–28°C
CP45	River	Lantz *et al*. (2021)	min. 4.5 mM			25°C

min., minimum; indicates the highest concentration tested.

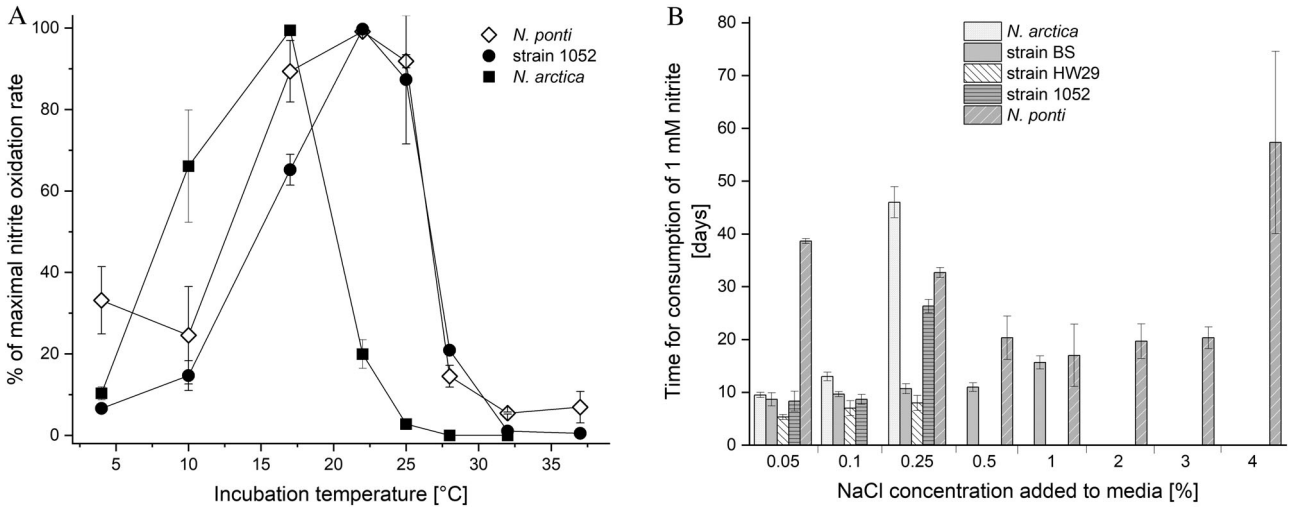

Fig. 2. Temperature optima and salt tolerance.
A. Nitrite oxidation of *N. ponti* M3, 1052 and *N. arctica* incubated at different temperatures, presented in percentages of the respective maximum oxidation rate. The connecting lines serve visualization purposes only.
B. Time required to oxidize 1 mM nitrite by *N. arctica*, 1052 (both from permafrost soil), *N. ponti* M5, HW29 (both from aquaculture) and BS (from WWTP) at increasing NaCl concentrations added to the media. Except for *N. ponti*, the experiment was terminated after 55 days. 0.1% was not tested on *N. ponti*. All experiments were conducted in triplicates, error bars show the standard deviation.

from eelgrass sediment. As mentioned above, adaptation of strain 1052 to climatic conditions prevailing at the time when the soil froze >3000 years ago might explain the preference for higher temperatures of this permafrost *Nitrotoga*.

Metagenomic sequencing and phylogenetic analyses of the Nitrotoga *enrichments*

The metagenomes of five *Nitrotoga* enrichments (*N. arctica* 6680, 1052, HW29, BS, *N. ponti* M5) were sequenced, assembled and binned, resulting in 1–9 metagenome-assembled genomes (MAGs) per culture. In each culture, *Nitrotoga* was the only known NOB based on taxonomic classification of all MAGs using GTDB-Tk (Supplementary Table S2). The *Nitrotoga* genomes were highly covered in all metagenomes, with a mean coverage ranging from 49.5 to 469.6. Based on metagenomic read recruitment for all assembled reads the strains constituted between 14.1% and 99.96% relative abundance in the enrichment cultures at the time of sequencing (Supplementary Table S3). Near-complete genomes of four strains were obtained by using Illumina MiSeq sequencing and the complete genome of *N. arctica* was assembled by using a hybrid assembly approach combining long- and short-read sequencing.

All obtained *Nitrotoga* MAGs represent high-quality genomes with an estimated genome completeness ≥95% and sizes of 2.99–3.45 Mbp containing 2774–3139

predicted coding sequences (Supplementary Table S3). Although only two MAGs included the complete set of rRNA genes, *Nitrotoga* 16S rRNA gene sequences were also identified in the unbinned fraction of the other cultures. The closed genome of *N. arctica* contained two identical sets of rRNA genes, similar to *N. fabula* and strain AMP-1 (Kitzinger *et al*., 2018; Ishii *et al*., 2020), and we thus assume that this is also the case for the other strains. While the five *Nitrotoga* strains had highly similar 16S rRNA genes (98.76%–99.6%), the highest average nucleotide identity (ANI) between these genomes was 90.54% for the permafrost soil strains *N. arctica* and strain 1052 (Supplementary Table S4) and thus below the species cutoff of 95% (Konstantinidis and Tiedje, 2005). The discrepancy between highly conserved 16S rRNA gene sequences and a pronounced genome-level variability was also described previously for *Nitrotoga* enrichments obtained from river sediment and water column samples (Boddicker and Mosier, 2018) and thus seems to represent a general feature in this genus. Phylogenomic analysis based on a concatenated alignment of 92 single-copy core genes revealed at least three main groups within the genus: a distinct clade of uncultured, aquatic MAGs with reduced genome sizes (<1.5 Mbp), *N. fabula*, which clustered separately, and a third clade comprising all other cultured *Nitrotoga* as well as uncultured MAGs from different environmental origins (Fig. 3). Except for *N. ponti* that clustered together with a MAG from a submarine oil seep, the phylogenomic analysis did not infer any clear patterns based on shared habitat type, which was also confirmed by 16S rRNA phylogeny (Supplementary Fig. S4).

A pangenome analysis of the five genomes obtained in this study and 10 additional, publicly available *Nitrotoga* genomes (Supplementary Table S5) included 42 049 genes summarized in 9443 gene clusters, of which 1080 formed the core genome, 3067 the variable genome (clusters shared by at least two but not all genomes) and 5296 gene clusters were detected in only one genome (singletons; Supplementary Table S6). The pangenome analysis revealed a strong conservation of metabolic key features, including the machineries for nitrite oxidation, respiration and CO_2 fixation as discussed in detail below (Fig. 4).

Nitrite oxidation

Nitrite oxidation, the catabolic key reaction in NOB, is catalysed by the NXR, a member of the type II DMSO reductase molybdopterin cofactor-binding enzyme family. Based on cellular localization, periplasmic and cytoplasmic NXR types can be defined, although also within these the nitrite oxidation machineries evolved independently in different taxonomic lineages (Lücker *et al*., 2010; Hemp *et al*., 2016; Kitzinger *et al*., 2018). The cytoplasmic NXR type, as shown for *Nitrobacter*, is membrane associated, whereas prediction suggests that the periplasmic type (e.g. in *Nitrospira* and *Nitrospina*) might occur as membrane-bound and/or soluble form (Spieck *et al*., 1998; Lücker *et al*., 2013; Mundinger *et al*., 2019). Notably, previous studies indicated that the NXR of *Nitrotoga* is only distantly related to the periplasmic NXR of *Nitrospira* and *Nitrospina* (Boddicker and Mosier, 2018; Kitzinger *et al*., 2018) and forms a distinct phylogenetic clade together with the thermophilic *Ca*. Nitrocaldera and *Ca*. Nitrotheca, both belonging to the phylum Chloroflexi (Supplementary Fig. S5) (Ishii *et al*., 2020; Spieck *et al*., 2020b).

Similar to other members of the type II DMSO reductase enzyme family, all known NXR complexes consist of at least two subunits. The substrate-binding alpha subunit (NxrA) catalyses the oxidation of nitrite to nitrate and shuttles the two obtained electrons to the beta subunit (NxrB). The electron transfer from NxrB to the respiratory chain is performed either directly using a yet unidentified electron carrier or via the gamma subunit (NxrC). All *Nitrospira*-type NxrA possess a twin-arginine secretion peptide for the translocation into the periplasm. NxrB, which lack signals for secretion, might be co-translocated together with NxrA (Lücker *et al*., 2010; Kitzinger *et al*., 2018). Notably, previous analyses suggested that the NxrC of *Nitrotoga* contains a secretory signal but no transmembrane helix and thus it was hypothesized that their NXR is a soluble periplasmic enzyme (Boddicker and Mosier, 2018; Kitzinger *et al*., 2018). In agreement with these previous predictions, also the NxrC sequences of the newly studied *Nitrotoga* genomes contained a signal peptide for Sec-dependent translocation but lacked transmembrane helices. Genes encoding the three NXR subunits (*nxrABC*) were located in a gene cluster together with a TorD-like chaperone that is putatively required for correct insertion of the molybdopterin cofactor into NxrA, similar to the role of the nitrate reductase chaperon NarJ (Blasco *et al*., 1998). Notably, the complete genomes of *N. fabula*, strain AMP1 and *N. arctica* contain two to three near-identical copies of the *nxr* gene cluster, potentially resulting in a gene dosage effect for rapid transcription (Kitzinger *et al*., 2018; Ishii *et al*., 2020, this study).

To confirm the prediction of a soluble periplasmic NXR, the NxrB-targeting monoclonal antibodies Hyb 153-3 (Bartosch *et al*., 1999) were used to investigate the cellular localization of this key enzyme in *Nitrotoga*. Previously, these antibodies were successfully applied in immunofluorescence labelling to confirm *Nitrotoga* as a novel NOB clade (Alawi *et al*., 2007).

Western blot analysis showed that the NxrB in *Nitrotoga arctica* is of the same size (46 kDa) as the

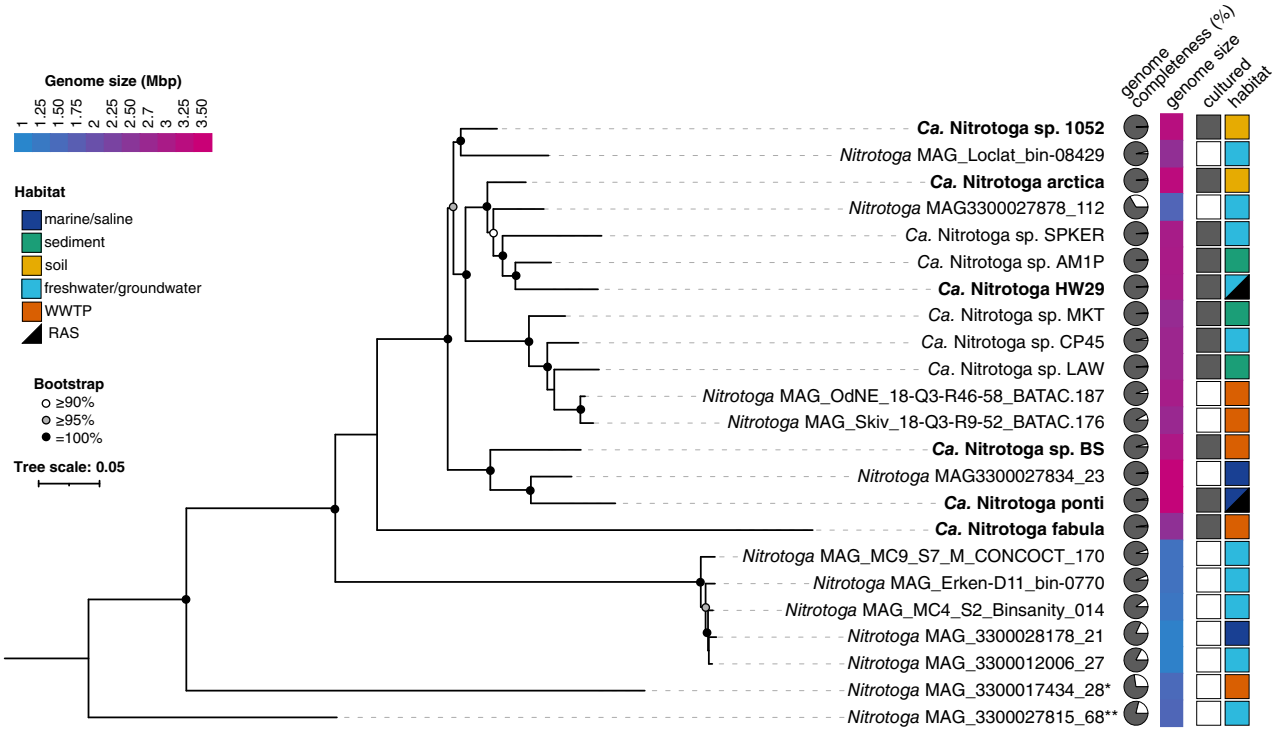

Fig. 3. Phylogenomic analysis of genome-sequenced *Nitrotoga*. The maximum likelihood tree is based on a concatenated alignment of 92 single-copy core genes containing 88 344 columns. Bootstrap support based on 1000 iterations is indicated by coloured circles. The matrix to the right indicates genome completeness, genome size, cultivation state (filled and open squares denote: cultivated and environmental strains, respectively) and source habitat. The scale bar indicates 0.05 amino acid substitutions per alignment position.

corresponding protein in *Nitrospira defluvii* A17 (Supplementary Fig. S6). Moreover, immunogold-labelling experiments with strains *N. arctica*, 1052 and HAM-1 confirmed that the NxrB is present in the periplasmic space and most probably soluble (Fig. 5A–D) since the gold particles were distributed throughout the wide periplasmic space. In control experiments without monoclonal antibodies, we observed only a few randomly distributed gold particles.

Interestingly, in the periplasmic space of a few cells of *Nitrotoga* strains Äspö and 1052 paracrystalline structures – highly ordered particles arranged in stacked rows – were observed (Fig. 5E and F). The size of a single particle was about 7–10 nm, matching the size of similar two-dimensional structures observed in *Nitrobacter* and *Nitrospira*, where these were membrane-bound and assumed to represent NXR (Spieck *et al*., 1996b; Spieck *et al*., 1998). In contrast to other NOB, these rows of particles in *Nitrotoga* are multilayered and further indicated a soluble nature of the NXR, as most of the stacked particles have no direct contact to the cytoplasmic membrane. Similarly, NXR particles in anammox bacteria of the genus *Kuenenia* appear to be organized in tubule-like structures located in the anammoxosome of the cells, where the energy delivering reactions take place (de Almeida *et al*., 2015; Chicano *et al*., 2021). In analogy, we suggest that the periplasm of *Nitrotoga* is an extended 'compartment' for energy conservation, especially considering that the NXR in anaerobic ammonium-oxidizing planctomycetes is more closely related to the periplasmic enzymes of *Nitrotoga*, *Nitrospira* and *Nitrospina*, than to the cytoplasm-oriented NXR-type of for instance *Nitrobacter* (Supplementary Fig. S5; Lücker *et al*., 2010).

Nitrogen metabolism

In addition to nitrite oxidation for energy conservation, many NOB can use nitrite as an N source for assimilation by reducing it to ammonia. Among the cultivated *Nitrotoga* strains, only strain BS requires external ammonium for reproducible growth (Wegen *et al*., 2019). This strain is the only cultured *Nitrotoga* lacking the *nasDE* genes encoding the assimilatory NAD(P)H-dependent nitrite reductase, and the formate/nitrite transporter gene (*focA*). Alternative nitrite reduction mechanisms, such as the ferredoxin-dependent nitrite reductase (NirA), the dissimilatory cytochrome *c* nitrite reductase (NrfA) and the octaheme nitrite reductase employed by some *Nitrospira*

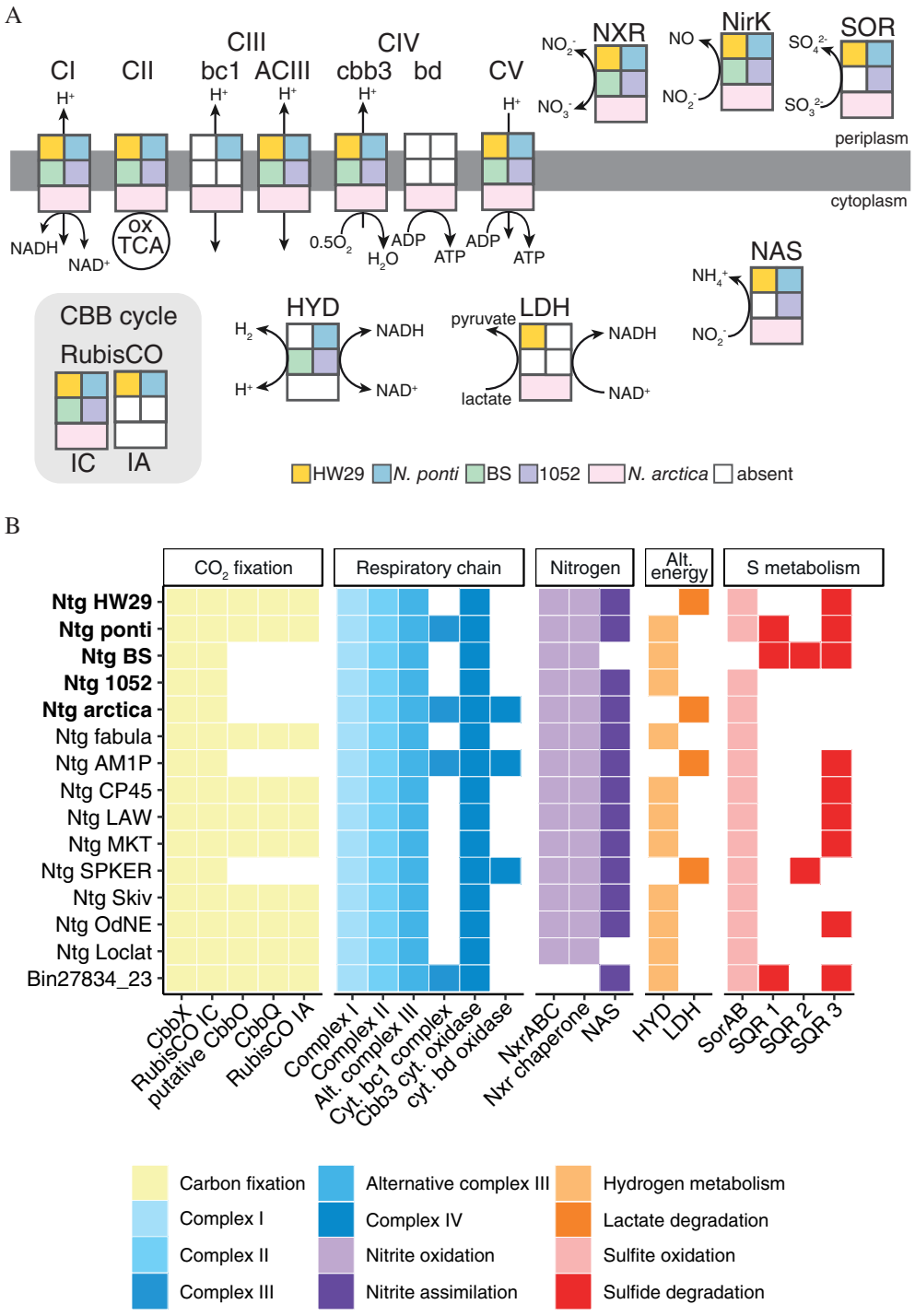

Fig. 4. Metabolic key features of the analysed *Nitrotoga* genomes.
A. Schematic summary of the metabolic potential of the five studied *Nitrotoga* strains.
B. Distribution patterns of metabolic key features in 15 high-quality *Nitrotoga* genomes. For detailed information see Tables S6 and S7. CI, complex I (NADH dehydrogenase); CII, complex II (succinate dehydrogenase); CIII, complex III (bc1, cytochrome bc_1 complex); ACIII, alternative complex III; CIV, complex IV (terminal oxidase); cbb3, Cytochrome cbb_3-type oxidase; bd, cytochrome *bd*-type oxidase; CV, complex V (ATP synthase); NXR, nitrite oxidoreductase; NirK, NO-forming nitrite reductase; SOR, sulfite:cytochrome *c* oxidoreductase; NAS, assimilatory nitrite reductase; LDH, lactate dehydrogenase; HYD, group 3d NAD-coupled [NiFe] hydrogenase; CBB cycle, Calvin-Benson-Bassham cycle; RuBisCO, ribulose-1,5-bisphosphate carboxylase/oxygenase; SQR, sulfide:quinone oxidoreductase; CbbO and CbbQ, putative RuBisCO-type IA activase; CbbX, RuBisCO-type IC activase.

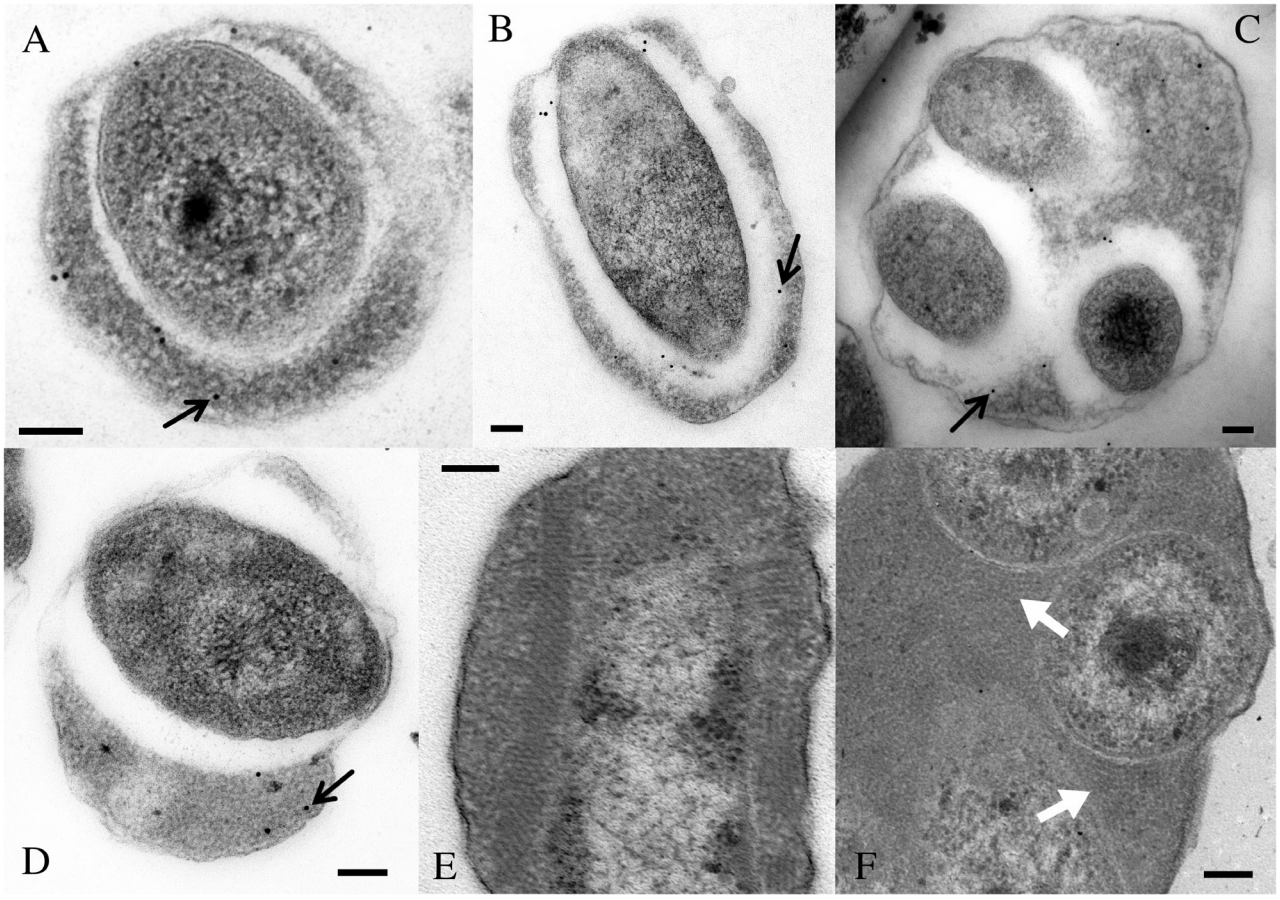

Fig. 5. Transmission electron micrographs of ultrathin sections.
(A, B) Cells of *N. arctica* 6680, (C) strain 1052 and (D) strain HAM-1, incubated with antibodies against the NXR ß-subunit and gold-labelled. Gold particles (round black dots of 10 nm, black arrows point out examples in each image) were visible inside the periplasmic space and only in few cases close to the cytoplasmic membrane.
(E, F) Cells of strain (e) Äspö terrace and (f) 1052, where arrays of crystalline proteins are visible as pairwise particles of 7–10 nm in the periplasm (white arrows). Scale bars correspond to 0.1 μm.

species (Koch *et al*., 2019) were also not identified in the BS genome. Similar to BS, the described nitrite-oxidizing Chloroflexi lack these genes and require ammonium supplementation for growth (Sorokin *et al*., 2012; Spieck *et al*., 2020a; Spieck *et al*., 2020b). The only nitrite-reducing enzyme encoded in the BS genome is the nitric oxide-forming nitrite reductase (NirK) that is conserved in most NOB. While the physiological role of NirK in *Nitrotoga* is still unclear, it was shown in *Nitrobacter* that NirK might be involved in maintaining the redox balance under low oxygen conditions (Starkenburg *et al*., 2008).

In contrast to other NOB that can produce ammonia by breaking down organic nitrogen compounds such as urea or cyanate (Koch *et al*., 2015; Palatinszky *et al*., 2015), genes for urea and cyanate degradation were not identified in any analysed *Nitrotoga* genome. However, all *Nitrotoga* encode a putative nitronate monooxygenase that might generate nitrite by oxidizing nitronates (Gadda and Francis, 2010; Salvi *et al*., 2014). In addition, some *Nitrotoga* possess a potential nitric oxide dioxygenase (HMP) to convert nitric oxide to nitrate as nitrosative stress response (Supplementary Table S7; Boddicker and Mosier, 2018).

Respiratory chain and carbon metabolism

Electrons from nitrite oxidation used for energy conservation are transferred to a high-affinity cbb_3-type cytochrome *c* oxidase, where they are used for oxygen reduction and the formation of proton motive force for ATP generation via the F_1F_o-type ATP synthase. Furthermore, *N. arctica* and strains SPKER and AM1P possess a cytochrome *bd*-type oxidase, which might be involved in respiration when using organics as electron donor or in oxidative and nitrosative stress defence (Boddicker and Mosier, 2018; Ishii *et al*., 2020). For anabolic processes, electrons are shuttled into the reverse electron transport chain that includes an alternative complex III (ACIII) and

a canonical NADH dehydrogenase. In addition to ACIII, a canonical cytochrome bc_1 complex was found in few *Nitrotoga* spp. (Fig. 4). Previously, in the proteome of the marine *Nitrospira marina* that also possesses both complex III types, only the cytochrome bc_1 complex was detected during nitrite-oxidizing conditions (Bayer *et al*., 2021). In contrast to *Nitrospira*, in *Nitrotoga* the ACIII appears to be the conserved complex III module, while the bc_1 complex is only found in some genomes. This suggests that ACIII has a crucial role in the respiratory chain of *Nitrotoga*. However, the exact metabolic functions of these different complex III types in NOB are yet unstudied and thus poorly understood. Lastly, all genome-analysed *Nitrotoga* possess the complete TCA cycle including a succinate dehydrogenase that also directly interacts with the quinone/quinol pool.

All five *Nitrotoga* genomes reported here contain all genes for the complete CBB cycle including a 'red' type IC ribulose-1,5-bisphosphate carboxylase/oxygenase (RuBisCO). Moreover, *N. ponti* and HW29 additionally possess a divergent copy representing the 'green' type IAq RuBisCO (Supplementary Fig. S7). The presence of two distinct RuBisCO enzymes was previously reported for few other *Nitrotoga* strains (Boddicker and Mosier, 2018; Kitzinger *et al*., 2018). Although also other autotrophic bacteria, including nitrite-oxidizing *Nitrobacter* spp. (Badger and Bek, 2008) possess multiple RuBisCO enzymes, it remains unclear whether these have different enzymatic characteristics, such as different affinities to CO_2 or O_2. No genes for carboxysome synthesis were identified in any investigated *Nitrotoga* genome, nor were such conspicuous compartments observed with electron microscopy of ultrathin cell sections. In contrast, for instance, *Nitrococcus mobilis*, *Nitrobacter agilis* and *Nitrosomonas eutropha*, which have an IAc RuBisCO, do produce carboxysomes (Shively *et al*., 1977; Badger and Bek, 2008). The lack of these CO_2-concentrating compartments in *Nitrotoga* indicates possible disadvantages at high oxygen concentrations, where the unwanted oxygenase function of RuBisCO may prevail. This might hint at a lifestyle adapted to low oxygen concentrations, which is in accordance with employing a high-affinity cbb_3 oxidase. Similar to their nitrite affinities, however, the oxygen affinities of *Nitrotoga* also seem lower than those of *Nitrospira* (Nowka *et al*., 2015a; Zheng *et al*., 2020).

Alternative energy metabolisms

In agreement with previous studies, the genus *Nitrotoga* seems to possess different metabolic capacities for energy conservation in addition to aerobic nitrite oxidation (Boddicker and Mosier, 2018; Kitzinger *et al*., 2018; Ishii *et al*., 2020). Namely, *Nitrotoga* might be able to oxidize hydrogen and lactate. Notably, these putative additional pathways of energy conservation were lacking in very streamlined *Nitrotoga* MAGs from the Great Lakes (Podowski *et al*., 2021). Some *Nitrotoga* spp. encode a group 3d NADH-coupled [NiFe] hydrogenase as well as respective accessory genes. The physiological role of this bidirectional hydrogenase in *Nitrotoga* still needs to be determined but might either be NAD^+-reduction using hydrogen as electron donor for aerobic or anaerobic respiration or hydrogen evolution for redox balancing in the presence of a suitable electron donor for growth. In addition, *Nitrotoga* sp. AMP1 as well as some other *Nitrotoga* possess a lactate dehydrogenase to reversibly convert lactate into pyruvate with NAD^+ as electron acceptor (Fig. 4; Ishii *et al*., 2020). In the presence of nitrite and lactate, a higher growth rate of *Nitrotoga* sp. AMP1 was observed compared to nitrite-only incubations, but the culture could not grow with lactate as the sole energy source (Ishii *et al*., 2020). Since increased nitrite oxidation rates were observed when pyruvate or catalase was added to the culture, the produced pyruvate from lactate conversion might also function as an H_2O_2 scavenger in AMP1 as shown for ammonia-oxidizing archaea (Kim *et al*., 2016; Ishii *et al*., 2020).

Genomic analyses indicated an ability to oxidize sulfur compounds within all investigated strains. While all strains except for BS possess a periplasmic sulfite dehydrogenase (SOR) for the oxidation of sulfite to sulfate, some genomes furthermore encode a sulfide:quinone oxidoreductase (SQR) for oxidation of hydrogen sulfide to elemental sulfur or polysulfide coupled to quinone reduction. In addition to energy conservation, SQR might also be involved in sulfide detoxification. Notably, strain BS possesses three different SQRs that are differently distributed in other *Nitrotoga* genomes (Fig. 4). Some of these *sqr* genes are located in close proximity of genes encoding rhodanese-like enzymes that together with a persulfide dioxygenase catalyse the production of sulfite to detoxify sulfide in heterotrophic bacteria (Xia *et al*., 2017). Thus, some *Nitrotoga* have a similar sulfur-metabolizing repertoire like *Nitrococcus mobilis*, a marine NOB reported to oxidize sulfide under oxic conditions (Füssel *et al*., 2017). While the exact role of these enzymes in *Nitrotoga* remains to be analysed, they might be especially beneficial in marine habitats, as due to the high concentrations of sulfate in seawater (28 mM), H_2S is readily produced in anaerobic sediment layers, and also under anaerobic or suboxic conditions in biofilters of marine RAS, with potential concentrations of >30 mg H_2S L^{-1} depending on salinity, pH and organic load (Rojas-Tirado *et al*., 2021). Therefore, H_2S might be a driving force for the abundance of *Nitrotoga* due to the higher tolerance level in comparison to *Nitrospira* in some systems (Delgado Vela *et al*., 2018).

Characterization of marine culture N. ponti

Since its discovery in 2007, detection of *Nitrotoga* in the nitrifying communities of communal and industrial WWTPs has increased significantly (Alawi *et al*., 2009; Lücker *et al*., 2015; Saunders *et al*., 2016; Figdore *et al*., 2018; Spieck *et al*., 2021). Contrastingly, only few findings in biofilters of RAS were reported, partly with *Nitrotoga* as most abundant NOB (Hüpeden *et al*., 2016; Navada *et al*., 2019; Pulkkinen, 2020). We detected *Nitrotoga*-like sequences also in biomass from RAS biofilters of an aquaculture research facility operated with North Sea water (Keuter *et al*., 2017), and as detailed above, the corresponding strain was subsequently enriched. The cells possess a similar morphology to those of *N. arctica* with the typical wide periplasmic space and form loose aggregates (Fig. 1D, Supplementary Fig. S1). *Nitrotoga ponti* showed high tolerances towards nitrite, nitrate (both at least 20 mM) and ammonium (at least 40 mM; Table 1 and S1, Fig. S3), and grows best at temperatures between 17°C and 25°C (Fig. 2A). A similarly high nitrite and nitrate tolerance as well as an optimum growth at relatively high temperatures were observed for *N. fabula* (Kitzinger *et al*., 2018). However, *N. fabula* is only distantly related to *N. ponti* and forms a phylogenetically distinct cluster and possesses the highest number of strain-specific genes (Fig. 3, Table S6). Instead, phylogenomic analyses showed that *N. ponti* clusters together with an environmental MAG obtained from a marine oil seep sample (Nayfach *et al*., 2020; Fig. 3). Generally, *Nitrotoga* seems to be rather rare in marine systems, as a global biogeographic analysis revealed that only 0.1% of marine metagenomic datasets contained *Nitrotoga*-like (≥97%) 16S rRNA gene sequences (Boddicker and Mosier, 2018). It will be of special interest to disclose the role of *Nitrotoga* in the oceans as well as in marine RAS in further studies. Interestingly, no *Nitrotoga* sequences were found in metagenomes from the same RAS several years after cultivation of *N. ponti* had started (Hüpeden *et al*., 2020), indicating either a temporal shift in NOB community or that *Nitrotoga* is merely introduced occasionally to this RAS with the make-up water and is not considerably growing in the system.

Nitrotoga ponti is not obligate marine but ceased almost all activity after a second transfer in non-marine media. Here, one of two parallel cultures oxidized 0.5 mM nitrite within 5 months. In a salt tolerance experiment it grew best at NaCl concentrations between 0.5% and 3%, while its congeners were sensitive towards elevated salt concentrations (Fig. 2B). The two strains from permafrost decreased activity already at 0.25% NaCl and strain HW29 ceased growth at 0.5%. Only strain BS grew well in up to 1% NaCl. Despite the fact that strain AM1 was isolated from coastal sediment (Ishii *et al*., 2017, 2020), it did not grow in salt concentrations >0.5%. Therefore, strain *N. ponti* represents the first enriched marine strain of this genus. However, also strain BS, which is affiliated with the same phylogenetic cluster as *N. ponti* (Fig. 3), seems to be more tolerant towards NaCl concentrations than the other non-marine strains (Fig. 2B).

Import or synthesis of different osmoprotectants and other physiological factors such as different ion transporters might facilitate this tolerance against high salt concentrations. Genes for trehalose synthesis from glycogen/maltose were found only in *N. ponti* and MAG 23 (Supplementary Fig. S8), while strain BS possesses all genes for the biosynthesis of the osmolyte (hydroxy)ectoine (*ectABCD*). The production of osmolytes is a commonly found feature of other marine and non-marine NOB (Lin, 1994; Bayer *et al*., 2021; Mueller *et al*., 2021) and trehalose is known as suitable cryoprotecting agent in many NOB (Vekeman *et al*., 2013). In addition to synthesizing osmolytes, strain BS as well as *N. ponti* and MAG 23 might import osmolytes using different transporters (Fig. S8). All other *Nitrotoga* genomes lack genes for biosynthesis of these osmolytes, but most genomes contain genes for a sodium:proton transporter (*nhaA*) and a regulatory system (*envZ*, *ompR*) to react on osmolarity stress.

In addition to salt tolerance, another adaptation to marine environments appears to be scavenging of B12 and its biosynthesis intermediates. While *N. ponti*, similar to *N. marina* (Bayer *et al*., 2021), can use different intermediates to synthesize B12 including cobyrinate, L-threonine phosphate and dimethylbenzimidazole, a product of the riboflavin metabolism, other *Nitrotoga* strains possess only few enzymes involved in B12 synthesis resulting in a potentially non-functional pathway. The structurally complex, cobalt-containing cofactor cobalamin is required by all microorganisms and produced by only few bacteria and archaea from diverse phyla, including ammonia-oxidizing archaea (Heal *et al*., 2017). In the ocean, close interactions between B12 producers and auxotrophs like microalgae are known (e.g. Croft *et al*., 2005). Cobalamin is a vital cofactor that might be also important in nitrogen transformations, physiological stress and ocean deoxygenation, as was shown with archaeal ammonia oxidizers (Heal *et al*., 2017). It is likely that *N. ponti*, similar to other marine NOB such as *Nitrospira* and *Nitrospina*, could be either scavengers of B12 or produces this vitamin from externally acquired intermediates (Ngugi *et al*., 2016; Park *et al*., 2020; Bayer *et al*., 2021; Mueller *et al*., 2021).

Description of 'Candidatus Nitrotoga ponti'

Pón´ti (L. gen. n. ponti of the sea, referring to the original habitat). Gram-negative short rods or coccoid cells forming loose colonies. Cells have wide irregularly shaped

periplasms and reach length of up to 1.3 μm. Non-motile. Aerobic chemolithoautotrophic nitrite oxidizer that uses carbon dioxide as sole carbon source. Non-obligate marine with optimum activity between 0.5% and 3% NaCl and 17°C–25°C. Nitrite oxidation was observed at concentrations up to 20 mM nitrite and 20 mM nitrate (higher concentrations not tested). The genome has a size of 3.45 Mb, with a GC content of 47.3 mol.% (chromosome). The '*Ca*. Nitrotoga ponti' strain M5 was isolated from biomass from a biofilter of a marine recirculation aquaculture facility in Büsum, Germany, which is operated with water from the North Sea.

Conclusions

In the present study, we expand the current knowledge about genomic, morphological and physiological features of the genus *Nitrotoga* by identifying common characteristics of these cold-adapted NOB. Additionally, some ultrastructural, as well as physiological peculiarities of distinct species, were observed. Such information can be useful in culture-dependent as well as culture-independent research aiming to further disclose the ecological roles in different habitats of this nitrite-oxidizing group. This is of special interest in the case of the first described marine *Nitrotoga* strain. With the genomic information obtained, physiological exploration regarding alternative metabolisms or auxotrophy should follow. For this, isolation efforts, possibly using approaches described here, in Kitzinger *et al*. (2018) or Ishii *et al*. (2017), need to be intensified, to isolate previously enriched strains as well as to obtain novel strains from a variety of ecosystems.

Experimental procedures

Strains and sampling

For comparison and to complement physiological and morphological descriptions we used the following published strains: *N*. *arctica*, the first described *Nitrotoga* strain. Here, we used highly enriched (98%) cultures 6680 and 6678, originating from adjoining soil samples from the active layer of permafrost affected soil in the Lena river delta (Alawi *et al*., 2007), cultivated at 17°C. HW29, a highly enriched (99%) strain from a rainbow trout RAS supplied with groundwater in northeast Germany (Hüpeden *et al*., 2016), cultivated at 17°C to 22°C. HAM-1 and BS, two cultures originate from activated sludge of the WWTP in Hamburg-Dradenau. Culture HAM-1 is the pre-culture of strain BS and was cultivated at 10°C (Alawi *et al*., 2009), strain BS was cultivated at 22°C and obtained an enrichment level of 87% (Wegen *et al*., 2019).

For additional enrichments of *Nitrotoga* the following samples were used: (i) In summer 2001, sample 1052 was taken from a permafrost soil core (horizon between 51 and 94 cm depth). The core was drilled on Kurungnakh Island, Russia (N 72°20′, E 126°17′), in the depression of a low-centred ice-wedge polygon (Bischoff *et al*., 2013). The permafrost table in this ice complex lay in a depth of 30 cm. The sandy soil sample had a pH of 5.5 and contained 110 μg NH_4^+, 0.8 μg NO_2^- and 5.5 μg NO_3^- g^{-1} dry weight. The soil in this layer was formed in the Middle to Late Holocene; the environment during this time has been described as warm and wet (Wetterich *et al*., 2008). (ii) The Äspö hard rock laboratory is an up to 500 m deep artificial tunnel system in iron-rich bedrock north of Oskarshamn, Sweden, with a temperature of 15°C (Ionescu *et al*., 2015). A sample was taken here in 2011 from a thick orange-brown biofilm in brackish meteorite and baltic water (4 mg L^{-1} NH_4, 0.185 ng L^{-1} NO_3) in 160 m depth. The sample was used to inoculate culture 'Äspö terrace'. (iii) Biocarriers from the moving bed bioreactor of two RAS (M3 and M5) of a marine aquaculture research facility (GMA, Gesellschaft für marine Aquakultur mbH) located on the North Sea coast in Büsum, Germany, were used to inoculate marine NOB medium (see Keuter *et al*., 2017, for RAS details).

Cultivation and physiological experiments

The *Nitrotoga* strains were grown in non-agitated 300 ml Erlenmeyer flasks kept in the dark in 100 to 150 ml mineral salts medium (Spieck and Lipski, 2011) or marine mineral salt medium (Watson and Waterbury, 1971) prepared with 70% seawater. The media were amended with 0.3 mM nitrite, which was replenished when consumed to keep the cells active and to increase cell density. Cells of the strain 1052 enrichment culture were separated by an optical tweezers system (PALM MicroTweezers, Carl Zeiss Microscopy GmbH, Munich, Germany) as described in Nowka *et al*. (2015b), and additionally through dilution series using mineral medium. The enrichments were checked by fluorescence *in situ* hybridization with *Nitrotoga*-specific probe Ntg122 and competitor probes as described in Lücker *et al*. (2015) or by amplicon sequencing of the 16S rRNA gene as described in Wegen *et al*. (2019). The absence of other known NOB was further confirmed in metagenomic analyses.

All physiological tests were carried out either in 300 ml Erlenmeyer flasks with 100 ml medium or test tubes with 10 ml medium in duplicates (ammonium, nitrite and nitrate tolerance) or triplicates (salt and temperature optima). To test tolerance limits, NH_4Cl, $NaNO_2$, $NaNO_3$ and NaCl were added in different concentrations. For salt tolerance, the medium for the marine strain was prepared with aqua dest. instead of seawater, without addition of

vitamins, but with marine stock solution (10×). The test media were inoculated with 1% (vol./vol.) active culture and incubated in the dark without agitation. The Griess-Ilosvay spot test (Schmidt and Belser, 1994) was used to determine when all nitrite was depleted. To calculate nitrification rates in the temperature test, samples were taken regularly, and nitrite and nitrate were analysed via ion-pair chromatography with a LiChrospher RP-18 column (125 by 4 mm; Merck, Germany) and UV detection in an automated system (Hitachi LaChrom Elite; VWR International, Darmstadt, Germany).

Transmission electron microscopy

For transmission electron microscopic observations, cells were collected by centrifugation and fixed in 2.5% glutaraldehyde for 1.5 h, followed by an overnight incubation in 2% osmium tetroxide (detailed in Spieck and Lipski, 2011). Fixed cells were embedded in Spurr resin (Spurr, 1969). Ultrathin sections were taken with a diamond knife, stained with uranyl acetate and lead citrate (Watson, 1958; Reynolds, 1963) and analysed using a transmission electron microscope (Zeiss model Leo 906E with a CCD camera model 794; Carl Zeiss, Jena, Germany).

Post-embedding labelling

Cells of *Nitrotoga* were fixed with 2.5% paraformaldehyde for 1 h on ice. After washing several times in cold PBS (pH 7.4) the cells were fixed with 0.05% osmium tetroxide overnight and dehydrated on ice with increasing concentrations of ethanol (15%–100%) in a modified version as described by Spieck *et al*., (1996a). Infiltration and embedding in London Resin White (Craig and Miller, 1984) was performed by mixing the cells in resin with ethanol (1:2, 1:1, 1:2 vol./vol.) for 2 h each and finally pure resin overnight. Ultrathin sections were collected on nickel grids, blocked with 1% BSA in PBS containing 10 mM glycine for 30 min and incubated with the monoclonal antibody Hyb 153-3 (Bartosch *et al*., 1999) in a dilution of 1:10 or 1:50 for 1 h at room temperature. Incubation with goat anti-mouse IgG-gold complexes (GAM; 10 nm) 1:100 for 2 h and post-staining were done as described by Spieck *et al*. (1996a). Partly, a post-fixation with 1% glutaraldehyde for 10 min was included. Counterstaining was performed with 1% aqueous uranyl acetate for 20 min and briefly with Reynold's lead citrate (Komis *et al*., 2006). In control experiments, incubation with the monoclonal antibodies was omitted.

Metagenome sequencing

For all metagenomes, DNA was extracted using the Ultra-Clean Microbial DNA Isolation Kit (MO BIO Laboratories, Carlsbad, USA). Sequencing libraries were prepared using the Nextera XT kit (Illumina, San Diego, USA) according to the manufacturer's protocols. For this, ≥1 ng DNA per sample was used for tagmentation. After addition of indexed adaptors and amplification of each library, the libraries were purified using AMPure XP beads (Beckman Coulter, Indianapolis, USA). Subsequent to checking quantity and size distribution using the Qubit high sensitivity dsDNA kit (Thermo Fisher Scientific, Waltham, USA) and Agilent 2100 Bioanalyzer (Agilent Technologies, Santa Clara, USA) respectively, the libraries were diluted to a final concentration of 4 nM, pooled in equimolar concentrations and denatured. The pooled libraries were paired-end sequenced (2 × 300 bp) on an Illumina MiSeq system using MiSeq reagent kit v3 (Illumina).

Assembly and binning

Adaptor removal and quality trimming of raw reads were performed using BBDUK BBTOOLS v.37.76 (https://jgi.doe.gov/data-and-tools/bbtools) with the following parameters: $k = 23$, mink = 11, hdist = 1, ktrim = r, qtrim = rl, trimq = 17, maq = 20, maxns = 0, minlen = 150, tossjunk = t, tbo. For each metagenome, trimmed reads were assembled using spades v3.14.0 (Nurk *et al*., 2017) with the metagenome option and default parameters. Except for HW29, automated binning was done using MetaBat2 (Kang *et al*., 2019) with following parameters: minimum contig length = 1000, minimum contig depth = 1 and minimum bin size = 0.5 Mbp. To obtain coverage data for binning, the trimmed reads were mapped onto the assembled contigs using Burros–Wheeler aligner BWA mem v.0.7.17-r1188 (Li and Durbin, 2010). Subsequent quality control and manual refinement of bins were done using anvi'o v.6.1 (Eren *et al*., 2015). For this, the assembly was filtered for a minimum contig length = 1000 and the trimmed reads were again mapped onto the assembled contigs using BWA mem v.0.7.17-r1188. The obtained coverage information, as well as automated binning results, were imported into the anvi'o contig database, which also includes all predicted open reading frames (ORFs) of the assembled contigs identified using prodigal (Hyatt *et al*., 2010). Single-copy core genes of archaea (Rinke *et al*., 2013) and bacteria (Campbell *et al*., 2013) were identified using HMMER (Eddy, 2011) and these single-copy core genes were compared to the GTDB-Tk database (Parks *et al*., 2018) for taxonomic classification. In addition, the ORFs were annotated using the Cluster of Orthologous Groups of proteins (COG) database. Subsequently, the anvi'o interactive

interface was employed to control the quality of automated bins and to manually refine them manually if needed. In addition, for BS, *N. ponti* and *N. arctica* 6680 the bin refinement tool 'anvi-refine' was employed to further improve the quality of the manually refined bin. For *N. ponti*, the 16S rRNA gene sequence was extracted from the assembly using 'anvi-get-sequences-for-hmm-hits' with the hmm search for 'Ribosomal_RNAs'. For HW29, manual binning using anvi'o was performed as described above without prior automated binning. Before and after the anvi'o workflow, quality and taxonomic affiliation of bins were analysed using the lineage workflow of CheckM v.1.0.11 (Parks *et al*., 2015) and the classify_wf workflow of GTDB-Tk v.0.3.2 (Parks *et al*., 2018) respectively.

Long-read sequencing and genome closure of N. arctica *6680*

For long-read Nanopore sequencing, the DNA library was constructed using 104 ng of DNA and the Ligation Sequencing Kit 1D (SQK-LSK109) and the Native Barcoding Expansion Kit (EXP-NBD114) according to the manufacturer's protocol (Oxford Nanopore Technologies). Subsequently, end repair of the fragments was performed using the NEBNext FFPE DNA Repair Mix (New England Biolabs, Ipswich, MA, USA). After purifying the fragments using AMPure XP beads (Beckman Coulter Life Sciences, Indianapolis, IN, USA), end repair and dA-tailing was performed using the NEBNext Ultra II End Repair/dA-Tailing Module (New England Biolabs). Subsequently, the fragments were purified using the AMPure XP beads and the DNA concentration of the library was quantified using the Qubit dsDNA HS Assay Kit. After ligation of adapters using the NEBNext® Quick Ligation Module (New England Biolabs), the library was purified using AMPure XP beads and loaded on a Flow cell (FLO-MIN106, Oxford Nanopore Technologies). The raw Nanopore fast5 data were basecalled using the basecaller guppy v.4.0.11 + f1071ce on a MinIon Mk1C sequencer (Oxford Nanopore Technologies).

Porechop v.0.2.3_seqan2.1.1 (https://github.com/rrwick/Porechop) with default settings was used for removing sequencing adapters and checking for chimaeric reads. Subsequently, the Nanopore reads were assembled using Canu v.1.8 (Koren *et al*., 2017) with following parameters: 'genomeSize = 50 m', 'corOutCoverage = 1000', 'useGrid = false', 'stopOnReadQuality = false', and 'stopOnLowCoverage = 5'. The resulting assembly was polished using Racon v.1.3.1 (Vaser *et al*., 2017) based on mapping the trimmed Nanopore sequencing reads onto the assembly using the default settings of minimap2 v.2.16-r922 (Li, 2018). The obtained closed genome of *N. arctica* was taxonomically classified using the classify_wf of GTDB-Tk v.0.3.2 (Parks *et al*., 2018). Subsequently, the trimmed Illumina reads were mapped against the closed genome via bbmap.sh v.37.76 min-id 0.8 (sourceforge.net/projects/bbmap/) to identify short reads derived from *N. arctica*. A hybrid assembly was performed using unicycler v.0.4.4 with the mapped Illumina reads and the polished long-read assembly as existing long-read assembly and the following parameters to identify *dnaA* as proxy for the origin of replication: 'start_gene_id 60' 'start_gene_cov 80' using DnaA of *Nitrotoga fabula* as reference (GenBank: SPS04574.1). This hybrid assembly approach resulted in a closed *N. arctica* 6680 genome whose taxonomic affiliation was again confirmed via GTDB-Tk v.0.3.2 (Parks *et al*., 2018) and that was further used in all analyses.

All five *Nitrotoga* genomes were gene-called and annotated via the genome annotation platform MicroScope (Vallenet *et al*., 2020). For selected genes, the annotation was refined manually as described previously (Kitzinger *et al*., 2018). For selected features, homologous proteins were identified using the phyloprofile tool implemented in the MicroScope platform with cut-offs of ≥50% identity and ≥80% query coverage (Supplementary Table S7). The cellular localization and putative transmembrane helixes of NXR proteins were predicted using the tools SignalP 5.0 and Phobius (Käll *et al*., 2004; Almagro Armenteros *et al*., 2019). For read recruitment analyses, all trimmed reads were mapped against the respective assemblies and the *Nitrotoga* genomes using bbmap.sh v.37.76 min-id 0.8 (sourceforge.net/projects/bbmap/) using: 'ambig=best minid=0.97 pairedonly=t' to report rpkm and number of mapped reads. The number of mapped reads was used to calculate the percentage of reads that mapped to the respective *Nitrotoga* genome of all reads mapped to the corresponding assembly.

Raw sequencing data (Illumina and NanoPore fastq) and the genome assemblies of the five *Nitrotoga* strains have been deposited in the European Nucleotide Archive under project PRJEB48217.

Phylogenomic analyses

For phylogenetic comparison of the five *Nitrotoga* enrichments, 36 *Nitrotoga* MAGs were downloaded from the NCBI assembly database, IMG/M and MAGE. Of these MAGs, 26 were classified as *Nitrotoga* based on GTDB R202 (Parks *et al*., 2021) and 10 by additional, previous studies (Nayfach *et al*., 2020; Singleton *et al*., 2021). Non-redundant medium quality genomes were selected by using the dereplicate workflow of dRep v2.4.2 (Olm *et al*., 2017) with default settings, but an estimated genome completion ≥50% and contamination of ≤10%.

The UBCG pipeline was used to extract and align 92 single-copy core genes from 23 *Nitrotoga* genomes that were published by Boddicker and Mosier (2018),

Kitzinger *et al*. (2018), Ishii *et al*. (2020), Nayfach *et al*. (2020), Buck *et al*. (2021), Podowski *et al*. (2021) and Singleton *et al*. (2021) (Supplementary Table S5) and two *Gallionellaceae* RefSeq assemblies (GCF_000974685.2 and GCF_000145255.1) as outgroup (Na *et al*., 2018). Based on the concatenated alignment comprising 88 344 columns, a maximum-likelihood phylogenomic tree was calculated using IQ-TREE 1.6.12 (Nguyen *et al*., 2015) via W-IQ-TREE (Trifinopoulos *et al*., 2016) with 1000 bootstrap replications and the integrated Modelfinder (Kalyaanamoorthy *et al*., 2017), which identified GTR + F + I + G4 as best-fitting substitution model.

Pangenome analysis

Based on their phylogenetic relatedness to the five *Nitrotoga* enrichements, 10 additional genomes with an estimated genome completeness ≥80% were included in the pangenome analysis (Supplementary Table S5). For *Nitrotoga fabula*, only the chromosome sequence was used for the analysis. For comparative genomics, the anvi'o pangenome workflow was followed as described by Delmont and Eren using anvi'o v6.1 (Delmont and Eren, 2018). All genomes were filtered to remove contigs ≤1000 bp and for each genome an anvi'o contig database was generated. ORFs were predicted using prodigal (Hyatt *et al*., 2010), single-copy core genes were identified using HMMER and genes were annotated using the COG and Pfam databases. Singletons, variable and core genes were identified via anvi-pan-genome with minbit parameter 0.5 and MCL-inflation 8, BLASTp to analyse sequence similarity, and Euclidean distance and Ward linkage for clustering. For combining the pangenome analysis results and the selected key feature table, gene sequences of all gene clusters of the pangenome were extracted and used as input for nucleotide BLAST databases for each genome separately via makeblastdb. The gene sequences of the corresponding MicroScope annotation (Vallenet *et al*., 2020) were used as a query for a BLASTn search against the corresponding BLAST database using the parameters 'evalue 1e-6' and 'max_target_seqs 10' and only hits with an identity ≥96% were kept for further analysis (Supplementary Table S7). ANI values were calculated via anvi-compute-genome-similarity using PyANI and ANIb for alignment (Pritchard *et al*., 2016).

Acknowledgements

The authors would like to thank Elke Woelken for excellent technical assistance in electron microscopy, as well as Christina Hartwig for the immunoblot analysis, Katharina Besler for cultivation of *Nitrotoga* from Äspö, and Theo van Alen and Geert Cremers for sequencing. We thank Eva-Maria Pfeiffer for providing the soil sample from Kurungnakh, Siberia. We thank Professor Wolfgang Liebl, Joachim Reitner and Christine Heim for providing us with an opportunity to work on Äspö samples, Katharina Kitzinger for fruitful discussions and Aharon Oren for taxonomical advice. The LABGeM (CEA/Genoscope & CNRS UMR8030), the France Génomique and French Bioinformatics Institute national infrastructures (funded as part of Investissement d'Avenir program managed by Agence Nationale pour la Recherche, contracts ANR-10-INBS-09 and ANR-11-INBS-0013) are acknowledged for support within the MicroScope annotation platform.

Funding

This work was funded by the Deutsche Forschungsgemeinschaft (projects DFG SP 667/10–1 + 2 and DFG SP 667/11 attributed to ES, and DFG FOR 571 attributed to NL); HK and SL were supported by the Netherlands Organization for Scientific Research (NWO; VI.Veni.192.086 and 016.Vidi.189.050 respectively). Enrichment of *Nitrotoga* sp. 1052 was funded by the BMBF Russian–German Cooperation 'Laptev Sea System: Process Studies on Permafrost Dynamics in the Laptev Sea'.

References

Abramov, A., Vishnivetskaya, T., and Rivkina, E. (2021) Are permafrost microorganisms as old as permafrost? *FEMS Microbiol Ecol* **97**: fiaa260.

Achberger, A.M., Christner, B.C., Michaud, A.B., Priscu, J. C., Skidmore, M.L., Vick-Majors, T.J., *et al*. (2016) Microbial community structure of subglacial lake Whillans, West Antarctica. *Front Microbiol* **7**: 1457.

Alawi, M., Lipski, A., Sanders, T., Pfeiffer E.-M., and Spieck, E. (2007) Cultivation of a novel cold-adapted nitrite oxidizing betaproteobacterium from the Siberian Arctic. *ISME J* **1**: 256–264.

Alawi, M., Off, S., Kaya, M., and Spieck, E. (2009) Temperature influences the population structure of nitrite-oxidizing bacteria in activated sludge. *Environ Microbiol Rep* **1**: 184–190.

Almagro Armenteros, J.J., Tsirigos, K.D., Sønderby, C.K., Petersen, T.N., Winther, O., Brunak, S., *et al*. (2019) SignalP 5.0 improves signal peptide predictions using deep neural networks. *Nat Biotechnol* **37**: 420–423.

Badger, M.R., and Bek, E.J. (2008) Multiple Rubisco forms in proteobacteria: their functional significance in relation to CO_2 acquisition by the CBB cycle. *J Exp Bot* **59**: 1525–1541.

Bartosch, S., Wolgast, I., Spieck, E., and Bock, E. (1999) Identification of nitrite-oxidizing bacteria with monoclonal antibodies recognizing the nitrite oxidoreductase. *Appl Environ Microbiol* **65**: 4126–4133.

Bayer, B., Saito, M.A., McIlvin, M.R., Lücker, S., Moran, D. M., Lankiewicz, T.S., *et al*. (2021) Metabolic versatility of the nitrite-oxidizing bacterium *Nitrospira marina* and its

proteomic response to oxygen-limited conditions. *ISME J* **15**: 1025–1039.
Berleman, J.E., and Kirby, J.R. (2009) Deciphering the hunting strategy of a bacterial wolfpack. *FEMS Microbiol Rev* **33**: 942–957.
Bischoff, J., Mangelsdorf, K., Gattinger, A., Schloter, M., Kurchatova, A.N., Herzschuh, U., and Wagner, D. (2013) Response of methanogenic archaea to Late Pleistocene and Holocene climate changes in the Siberian Arctic. *Global Biogeochem Cycles* **27**: 305–317.
Blasco, F., Dos Santos, J.-P., Magalon, A., Frixon, C., Guigliarelli, B., Santini, C.-L., and Giordano, G. (1998) NarJ is a specific chaperone required for molybdenum cofactor assembly in nitrate reductase A of *Escherichia coli*. *Mol Microbiol* **28**: 435–447.
Boddicker, A.M., and Mosier, A.C. (2018) Genomic profiling of four cultivated *Candidatus* Nitrotoga spp. predicts broad metabolic potential and environmental distribution. *ISME J* **12**: 2864–2882.
Buck, M., Garcia, S.L., Fernandez, L., Martin, G., Martinez-Rodriguez, G.A., Saarenheimo, J., *et al*. (2021) Comprehensive dataset of shotgun metagenomes from oxygen stratified freshwater lakes and ponds. *Sci Data* **8**: 131.
Campbell, J.H., O'Donoghue, P., Campbell, A.G., Schwientek, P., Sczyrba, A., Woyke, T., *et al*. (2013) UGA is an additional glycine codon in uncultured SR1 bacteria from the human microbiota. *Proc Natl Acad Sci U S A* **110**: 5540–5545.
Chicano, T.M., Dietrich, L., de Almeida, N.M., Akram, M., Hartmann, E., Leidreiter, F., *et al*. (2021) Structural and functional characterization of the intracellular filament-forming nitrite oxidoreductase multiprotein complex. *Nat Microbiol* **6**: 1129–1139.
Christner, B.C., Priscu, J.C., Achberger, A.M., Barbante, C., Carter, S.P., Christianson, K., *et al*. (2014) A microbial ecosystem beneath the West Antarctic ice sheet. *Nature* **512**: 310–313.
Cornelissen, R., Bøggild, A., Thiruvallur Eachambadi, R., Koning, R.I., Kremer, A., Hidalgo-Martinez, S., *et al*. (2018) The cell envelope structure of cable bacteria. *Front Microbiol* **9**: 3044.
Craig, S., and Miller, C. (1984) LR white resin and improved on-grid immunogold detection of vicilin, a pea seed storage protein. *Cell Biol Int Rep* **8**: 879–886.
Croft, M.T., Lawrence, A.D., Raux-Deery, E., Warren, M.J., and Smith, A.G. (2005) Algae acquire vitamin B12 through a symbiotic relationship with bacteria. *Nature* **438**: 90–93.
Daims, H., Lücker, S., Le Paslier, D., and Wagner, M. (2011) Diversity, environmental genomics, and ecophysiology of nitrite-oxidizing bacteria. In *Nitrification (Wiley Online Books)*, Ward, B.B., Arp, D.J., and Klotz, M.G. (eds). London, UK: IWA Publishing, pp. 295–322.
Daims, H., Lücker, S., and Wagner, M. (2016) A new perspective on microbes formerly known as nitrite-oxidizing bacteria. *Trends Microbiol* **24**: 699–712.
de Almeida, N.M., Neumann, S., Mesman, R.J., Ferousi, C., Keltjens, J.T., Jetten, M.S.M., *et al*. (2015) Immunogold localization of key metabolic enzymes in the anammoxosome and on the tubule-like structures of *Kuenenia stuttgartiensis*. *J Bacteriol* **197**: 2432–2441.
Delgado Vela, J., Dick, G.J., and Love, N.G. (2018) Sulfide inhibition of nitrite oxidation in activated sludge depends on microbial community composition. *Water Res* **138**: 241–249.
Delmont, T.O., and Eren, A.M. (2018) Linking pangenomes and metagenomes: the *Prochlorococcus* metapangenome. *PeerJ* **6**: e4320.
Eddy, S.R. (2011) Accelerated profile HMM searches. *PLoS Comput Biol* **7**: e1002195.
Eren, A.M., Esen, O.C., Quince, C., Vineis, J.H., Morrison, H.G., Sogin, M.L., and Delmont, T.O. (2015) Anvi'o: An advanced analysis and visualization platformfor 'omics data. *PeerJ* **2015**: e1319.
Fan, L., Song, C., Meng, S., Qiu, L., Zheng, Y., Wu, W., *et al*. (2016) Spatial distribution of planktonic bacterial and archaeal communities in the upper section of the tidal reach in Yangtze River. *Sci Rep* **6**: 39147.
Figdore, B.A., Stensel, H.D., and Winkler, M.K.H. (2018) Bioaugmentation of sidestream nitrifying-denitrifying phosphorus-accumulating granules in a low-SRT activated sludge system at low temperature. *Water Res* **135**: 241–250.
Füssel, J., Lücker, S., Yilmaz, P., Nowka, B., van Kessel, M. A.H.J., Bourceau, P., *et al*. (2017) Adaptability as the key to success for the ubiquitous marine nitrite oxidizer *Nitrococcus*. *Sci Adv* **3**: e1700807.
Gadda, G., and Francis, K. (2010) Nitronate monooxygenase, a model for anionic flavin semiquinone intermediates in oxidative catalysis. *Arch Biochem Biophys* **493**: 53–61.
Haaijer, S.C.M., Ji, K., van Niftrik, L., Hoischen, A., Speth, D., Jetten, M.S.M., *et al*. (2013) A novel marine nitrite-oxidizing *Nitrospira* species from Dutch coastal North Sea water. *Front Microbiol* **4**: 60.
Heal, K.R., Qin, W., Ribalet, F., Bertagnolli, A.D., Coyote-Maestas, W., Hmelo, L.R., *et al*. (2017) Two distinct pools of B12 analogs reveal community interdependencies in the ocean. *Proc Natl Acad Sci U S A* **114**: 364–369.
Hemp, J., Lücker, S., Schott, J., Pace, L.A., Johnson, J.E., Schink, B., *et al*. (2016) Genomics of a phototrophic nitrite oxidizer: insights into the evolution of photosynthesis and nitrification. *ISME J* **10**: 2669–2678.
Hüpeden, J., Wegen, S., Off, S., Lücker, S., Bedarf, Y., Daims, H., *et al*. (2016) Relative abundance of *Nitrotoga* spp. in a biofilter of a cold-freshwater aquaculture plant appears to be stimulated by slightly acidic pH. *Appl Environ Microbiol* **82**: 1838–1845.
Hüpeden, J., Wemheuer, B., Indenbirken, D., Schulz, C., and Spieck, E. (2020) Taxonomic and functional profiling of nitrifying biofilms in freshwater, brackish and marine RAS biofilters. *Aquac Eng* **90**: 102094.
Hyatt, D., Chen, G.-L., Locascio, P.F., Land, M.L., Larimer, F.W., and Hauser, L.J. (2010) Prodigal: prokaryotic gene recognition and translation initiation site identification. *BMC Bioinformatics* **11**: 119.
Ionescu, D., Heim, C., Polerecky, L., Ramette, A., Haeusler, S., Bizic-Ionescu, M., *et al*. (2015) Diversity of iron oxidizing and reducing bacteria in flow reactors in the Äspö hard rock laboratory. *Geomicrobiol J* **32**: 207–220.
Ishii, K., Fujitani, H., Sekiguchi, Y., and Tsuneda, S. (2020) Physiological and genomic characterization of a new

'*Candidatus* Nitrotoga' isolate. *Environ Microbiol* **22**: 2365–2382.

Ishii, K., Fujitani, H., Soh, K., Nakagawa, T., Takahashi, R., and Tsuneda, S. (2017) Enrichment and physiological characterization of a cold-adapted nitrite-oxidizing Nitrotoga sp. from an eelgrass sediment. *Appl Environ Microbiol* **83**: e00549-17.

Justice, S.S., Hunstad, D.A., Cegelski, L., and Hultgren, S.J. (2008) Morphological plasticity as a bacterial survival strategy. *Nat Rev Microbiol* **6**: 162–168.

Käll, L., Krogh, A., and Sonnhammer, E.L.L. (2004) A combined transmembrane topology and signal peptide prediction method. *J Mol Biol* **338**: 1027–1036.

Kalyaanamoorthy, S., Minh, B.Q., Wong, T.K.F., von Haeseler, A., and Jermiin, L.S. (2017) ModelFinder: fast model selection for accurate phylogenetic estimates. *Nat Methods* **14**: 587–589.

Kang, D.D., Li, F., Kirton, E., Thomas, A., Egan, R., An, H., and Wang, Z. (2019) MetaBAT 2: an adaptive binning algorithm for robust and efficient genome reconstruction from metagenome assemblies. *PeerJ* **7**: e7359.

Karkman, A., Mattila, K., Tamminen, M., and Virta, M. (2011) Cold temperature decreases bacterial species richness in nitrogen-removing bioreactors treating inorganic mine waters. *Biotechnol Bioeng* **108**: 2876–2883.

Keuter, S., Beth, S., Quantz, G., Schulz, C., and Spieck, E. (2017) Longterm monitoring of nitrification and nitrifying communities during biofilter activation of two marine recirculation aquaculture systems (RAS). *Int J Aquac Fish Sci* **3**: 51–61.

Keuter, S., Kruse, M., Lipski, A., and Spieck, E. (2011) Relevance of *Nitrospira* for nitrite oxidation in a marine recirculation aquaculture system and physiological features of a *Nitrospira marina*-like isolate. *Environ Microbiol* **13**: 2536–2547.

Kim, J.G., Park, S.J., Sinninghe Damsté, J.S., Schouten, S., Rijpstra, W.I.C., Jung, M.Y., *et al*. (2016) Hydrogen peroxide detoxification is a key mechanism for growth of ammonia-oxidizing archaea. *Proc Natl Acad Sci U S A* **113**: 7888–7893.

Kitzinger, K., Koch, H., Lücker, S., Sedlacek, C.J., Herbold, C., Schwarz, J., *et al*. (2018) Characterization of the first "*Candidatus Nitrotoga*" isolate reveals metabolic versatility and separate evolution of widespread nitrite-oxidizing bacteria. *MBio* **9**: e01186-18.

Koch, H., Lücker, S., Albertsen, M., Kitzinger, K., Herbold, C., Spieck, E., *et al*. (2015) Expanded metabolic versatility of ubiquitous nitrite-oxidizing bacteria from the genus *Nitrospira*. *Proc Natl Acad Sci U S A* **112**: 11371–11376.

Koch, H., van Kessel, M.A.H.J., and Lücker, S. (2019) Complete nitrification: insights into the ecophysiology of comammox *Nitrospira*. *Appl Microbiol Biotechnol* **103**: 177–189.

Komis, G., Quader, H., Galatis, B., and Apostolakos, P. (2006) Macrotubule-dependent protoplast volume regulation in plasmolysed root-tip cells of *Triticum turgidum*: involvement of phospholipase D. *New Phytol* **171**: 737–750.

Konstantinidis, K.T., and Tiedje, J.M. (2005) Genomic insights that advance the species definition for prokaryotes. *Proc Natl Acad Sci U S A* **102**: 2567–2572.

Koren, S., Walenz, B.P., Berlin, K., Miller, J.R., Bergman, N. H., and Phillippy, A.M. (2017) Canu: scalable and accurate long-read assembly via adaptive k-mer weighting and repeat separation. *Genome Res* **27**: 722–736.

Lantz, M.A., Boddicker, A.M., Kain, M.P., Berg, O.M.C., Wham, C.D., and Mosier, A.C. (2021) Physiology of the nitrite-oxidizing bacterium *Candidatus* Nitrotoga sp. CP45 enriched from a Colorado River. *Front Microbiol* **12**: 2257.

Li, H. (2018) Minimap2: pairwise alignment for nucleotide sequences. *Bioinformatics* **34**: 3094–3100.

Li, H., and Durbin, R. (2010) Fast and accurate long-read alignment with Burrows–Wheeler transform. *Bioinformatics* **26**: 589–595.

Lin, L. (1994) Kompatible solute in nitrifizierenden Bakterien. Dissertation. University of Hamburg.

Liu, W., Yang, D., Chen, W., and Gu, X. (2017) High-throughput sequencing-based microbial characterization of size fractionated biomass in an anoxic anammox reactor for low-strength wastewater at low temperatures. *Bioresour Technol* **231**: 45–52.

Liu, Y., Li, S., Ni, G., Duan, H., Huang, X., Yuan, Z., and Zheng, M. (2021) Temperature variations shape niche occupation of *Nitrotoga*-like bacteria in activated sludge. *ACS ES&T Water* **1**: 167–174.

Lücker, S., Nowka, B., Rattei, T., Spieck, E., and Daims, H. (2013) The genome of *Nitrospina gracilis* illuminates the metabolism and evolution of the major marine nitrite oxidizer. *Front Microbiol* **4**: 27.

Lücker, S., Schwarz, J., Gruber-Dorninger, C., Spieck, E., Wagner, M., and Daims, H. (2015) *Nitrotoga*-like bacteria are previously unrecognized key nitrite oxidizers in full-scale wastewater treatment plants. *ISME J* **9**: 708–720.

Lücker, S., Wagner, M., Maixner, F., Pelletier, E., Koch, H., Vacherie, B., *et al*. (2010) A *Nitrospira* metagenome illuminates the physiology and evolution of globally important nitrite-oxidizing bacteria. *Proc Natl Acad Sci U S A* **107**: 13479–13484.

Lyons, N.A., and Kolter, R. (2015) On the evolution of bacterial multicellularity. *Curr Opin Microbiol* **24**: 21–28.

Ma, B., Yang, L., Wang, Q., Yuan, Z., Wang, Y., and Peng, Y. (2017) Inactivation and adaptation of ammonia-oxidizing bacteria and nitrite-oxidizing bacteria when exposed to free nitrous acid. *Bioresour Technol* **245**: 1266–1270.

Mariscal, V., Herrero, A., and Flores, E. (2007) Continuous periplasm in a filamentous, heterocyst-forming cyanobacterium. *Mol Microbiol* **65**: 1139–1145.

Moyer, C.L., Collins, R.E, and Morita, R.Y. (2017) Psychrophiles and psychrotrophs. In *Reference Module in Life Sciences*, Moyer, C.L., Collins, R.E., and Morita, R.Y. (eds). Amsterdam: Elsevier, pp. 1–12.

Mueller, A.J., Jung, M.-Y., Strachan, C.R., Herbold, C.W., Kirkegaard, R.H., Wagner, M., and Daims, H. (2021) Genomic and kinetic analysis of novel *Nitrospinae* enriched by cell sorting. *ISME J* **15**: 732–745.

Mundinger, A.B., Lawson, C.E., Jetten, M.S.M., Koch, H., and Lücker, S. (2019) Cultivation and transcriptional analysis of a canonical *Nitrospira* under stable growth conditions. *Front Microbiol* **10**: 1325.

Na, S.-I., Kim, Y.O., Yoon, S.-H., Ha, S., Baek, I., and Chun, J. (2018) UBCG: up-to-date bacterial core gene set

and pipeline for phylogenomic tree reconstruction. *J Microbiol* **56**: 280–285.
Navada, S., Vadstein, O., Tveten, A.-K., Verstege, G.C., Terjesen, B.F., Mota, V.C., *et al*. (2019) Influence of rate of salinity increase on nitrifying biofilms. *J Clean Prod* **238**: 117835.
Nayfach, S., Roux, S., Seshadri, R., Udwary, D., Varghese, N., Schulz, F., *et al*. (2020) A genomic catalog of Earth's microbiomes. *Nat Biotechnol* **39**: 499–509.
Ngugi, D.K., Blom, J., Stepanauskas, R., and Stingl, U. (2016) Diversification and niche adaptations of *Nitrospina*-like bacteria in the polyextreme interfaces of Red Sea brines. *ISME J* **10**: 1383–1399.
Nguyen, L.-T., Schmidt, H.A., von Haeseler, A., and Minh, B. Q. (2015) IQ-TREE: a fast and effective stochastic algorithm for estimating maximum-likelihood phylogenies. *Mol Biol Evol* **32**: 268–274.
Nowka, B., Daims, H., and Spieck, E. (2015a) Comparison of oxidation kinetics of nitrite-oxidizing bacteria: nitrite availability as a key factor in niche differentiation. *Appl Environ Microbiol* **81**: 745–753.
Nowka, B., Off, S., Daims, H., and Spieck, E. (2015b) Improved isolation strategies allowed the phenotypic differentiation of two *Nitrospira* strains from widespread phylogenetic lineages. *FEMS Microbiol Ecol* **91**: fiu031.
Nurk, S., Meleshko, D., Korobeynikov, A., and Pevzner, P.A. (2017) metaSPAdes: a new versatile metagenomic assembler. *Genome Res* **27**: 824–834.
Off, S., Alawi, M., and Spieck, E. (2010) Enrichment and physiological characterization of a novel *Nitrospira*-like bacterium obtained from a marine sponge. *Appl Environ Microbiol* **76**: 4640–4646.
Olm, M.R., Brown, C.T., Brooks, B., and Banfield, J.F. (2017) dRep: a tool for fast and accurate genomic comparisons that enables improved genome recovery from metagenomes through de-replication. *ISME J* **11**: 2864–2868.
Oren, A., Garrity, G., Parker, C., Chuvochina, M., and Trujillo, M. (2020) Lists of names of prokaryotic Candidatus taxa. *Int J Syst Evol Microbiol* **70**: 1466–5034.
Palatinszky, M., Herbold, C., Jehmlich, N., Pogoda, M., Han, P., von Bergen, M., *et al*. (2015) Cyanate as an energy source for nitrifiers. *Nature* **524**: 105–108.
Park, S.-J., Andrei, A.-Ş., Bulzu, P.-A., Kavagutti, V.S., Ghai, R., and Mosier, A.C. (2020) Expanded diversity and metabolic versatility of marine nitrite-oxidizing bacteria revealed by cultivation- and genomics-based approaches. *Appl Environ Microbiol* **86**: e01667-20.
Parks, D.H., Chuvochina, M., Rinke, C., Mussig, A.J., Chaumeil, P.-A., and Hugenholtz, P. (2021) GTDB: an ongoing census of bacterial and archaeal diversity through a phylogenetically consistent, rank normalized and complete genome-based taxonomy. *Nucleic Acids Res* **50**: D785–D794.
Parks, D.H., Chuvochina, M., Waite, D.W., Rinke, C., Skarshewski, A., Chaumeil, P.A., and Hugenholtz, P. (2018) A standardized bacterial taxonomy based on genome phylogeny substantially revises the tree of life. *Nat Biotechnol* **36**: 996.
Parks, D.H., Imelfort, M., Skennerton, C.T., Hugenholtz, P., and Tyson, G.W. (2015) CheckM: assessing the quality of microbial genomes recovered from isolates, single cells, and metagenomes. *Genome Res* **25**: 1043–1055.
Pester, M., Maixner, F., Berry, D., Rattei, T., Koch, H., Lücker, S., *et al*. (2014) NxrB encoding the beta subunit of nitrite oxidoreductase as functional and phylogenetic marker for nitrite-oxidizing *Nitrospira*. *Environ Microbiol* **16**: 3055–3071.
Philips, S., Laanbroek, H.J., and Verstraete, W. (2002) Origin, causes and effects of increased nitrite concentrations in aquatic environments. *Rev Environ Sci Biotechnol* **1**: 115–141.
Podowski, J.C., Paver, S.F., Newton, R.J., and Colemana, M.L. (2021) Genome streamlining, proteorhodopsin, and organic nitrogen metabolism in freshwater nitrifiers. *bioRxiv* 2021.01.19.427344.
Pritchard, L., Glover, R.H., Humphris, S., Elphinstone, J.G., and Toth, I.K. (2016) Genomics and taxonomy in diagnostics for food security: soft-rotting enterobacterial plant pathogens. *Anal Methods* **8**: 12–24.
Pulkkinen, J. (2020) Microbiology of biological filters in recirculating aquaculture systems. Dissertation. University of Jyväskylä.
Reynolds, E.S. (1963) The use of lead citrate at high pH as an electron-opaque stain in electron microscopy. *J Cell Biol* **17**: 208–212.
Rinke, C., Schwientek, P., Sczyrba, A., Ivanova, N.N., Anderson, I.J., Cheng, J.-F., *et al*. (2013) Insights into the phylogeny and coding potential of microbial dark matter. *Nature* **499**: 431–437.
Rojas-Tirado, P., Aalto, S.L., Åtland, Å., and Letelier-Gordo, C. (2021) Biofilters are potential hotspots for H2S production in brackish and marine water RAS. *Aquaculture* **536**: 736490.
Salvi, F., Agniswamy, J., Yuan, H., Vercammen, K., Pelicaen, R., Cornelis, P., *et al*. (2014) The combined structural and kinetic characterization of a bacterial nitronate monooxygenase from *Pseudomonas aeruginosa* PAO1 establishes NMO class I and II. *J Biol Chem* **289**: 23764–23775.
Sanders, T., Fiencke, C., Hüpeden, J., Pfeiffer, E.M., and Spieck, E. (2019) Cold adapted *Nitrosospira* sp.: a potential crucial contributor of ammonia oxidation in cryosols of permafrost-affected landscapes in Northeast Siberia. *Microorganisms* **7**: 699.
Saunders, A.M., Albertsen, M., Vollertsen, J., and Nielsen, P.H. (2016) The activated sludge ecosystem contains a core community of abundant organisms. *ISME J* **10**: 11–20.
Schmidt, E.L., and Belser, L.W. (1994) Autotrophic nitrifying bacteria. In *Methods of Soil Analysis*, Weaver, R., Angle, J., and Bottomley, P. (eds). Madison, WI: Soil Science Society of America, pp. 159–177.
Schmidt, S.K., Nemergut, D.R., Miller, A.E., Freeman, K.R., King, A.J., and Seimon, A. (2009) Microbial activity and diversity during extreme freeze–thaw cycles in periglacial soils, 5400 m elevation, Cordillera Vilcanota, Perú. *Extremophiles* **13**: 807–816.
Shively, J.M., Bock, E., Westphal, K., and Cannon, G.C. (1977) Icosahedral inclusions (carboxysomes) of *Nitrobacter agilis*. *J Bacteriol* **132**: 673–675.

Singleton, C.M., Petriglieri, F., Kristensen, J.M., Kirkegaard, R.H., Michaelsen, T.Y., Andersen, M.H., *et al*. (2021) Connecting structure to function with the recovery of over 1000 high-quality metagenome-assembled genomes from activated sludge using long-read sequencing. *Nat Commun* **12**: 2009.

Sorokin, D.Y., Lücker, S., Vejmelkova, D., Kostrikina, N.A., Kleerebezem, R., Rijpstra, W.I.C., *et al*. (2012) Nitrification expanded: discovery, physiology and genomics of a nitrite-oxidizing bacterium from the phylum Chloroflexi. *ISME J* **6**: 2245–2256.

Spieck, E., Aamand, J., Bartosch, S., and Bock, E. (1996a) Immunocytochemical detection and location of the membrane-bound nitrite oxidoreductase in cells of *Nitrobacter* and *Nitrospira*. *FEMS Microbiol Lett* **139**: 71–76.

Spieck, E., Ehrich, S., Aamand, J., and Bock, E. (1998) Isolation and immunocytochemical location of the nitrite-oxidizing system in *Nitrospira moscoviensis*. *Arch Microbiol* **169**: 225–230.

Spieck, E., and Lipski, A. (2011) Cultivation, growth physiology, and chemotaxonomy of nitrite-oxidizing bacteria. In *Methods in Enzymology*, Klotz, M.G. (ed). Burlington: Academic Press, pp. 109–130.

Spieck, E., Müller, S., Engel, A., Mandelkow, E., Patel, H., and Bock, E. (1996b) Two-dimensional structure of membrane-bound nitrite oxidoreductase from *Nitrobacter hamburgensis*. *J Struct Biol* **117**: 117–123.

Spieck, E., Sass, K., Keuter, S., Hirschmann, S., Spohn, M., Indenbirken, D., *et al*. (2020a) Defining culture conditions for the hidden nitrite-oxidizing bacterium *Nitrolancea*. *Front Microbiol* **11**: 1522.

Spieck, E., Spohn, M., Wendt, K., Bock, E., Shively, J., Frank, J., *et al*. (2020b) Extremophilic nitrite-oxidizing Chloroflexi from Yellowstone hot springs. *ISME J* **14**: 364–379.

Spieck, E., Wegen, S., and Keuter, S. (2021) Relevance of *Candidatus* Nitrotoga for nitrite oxidation in technical nitrogen removal systems. *Appl Microbiol Biotechnol* **105**: 7123–7139.

Spurr, A.R. (1969) A low-viscosity epoxy resin embedding medium for electron microscopy. *J Ultrastruct Res* **26**: 31–43.

Starkenburg, S.R., Larimer, F.W., Stein, L.Y., Klotz, M.G., Chain, P.S., Sayavedra-Soto, L.A., *et al*. (2008) Complete genome sequence of Nitrobacter hamburgensis X14 and comparative genomic analysis of species within the genus *Nitrobacter*. *Appl Environ Microbiol* **74**: 2852–2863.

Tecon, R., and Leveau, J.H.J. (2016) Symplasmata are a clonal, conditional, and reversible type of bacterial multicellularity. *Sci Rep* **6**: 31914.

Trifinopoulos, J., Nguyen, L.-T., von Haeseler, A., and Minh, B.Q. (2016) W-IQ-TREE: a fast online phylogenetic tool for maximum likelihood analysis. *Nucleic Acids Res* **44**: W232–W235.

Vallenet, D., Calteau, A., Dubois, M., Amours, P., Bazin, A., Beuvin, M., *et al*. (2020) MicroScope: an integrated platform for the annotation and exploration of microbial gene functions through genomic, pangenomic and metabolic comparative analysis. *Nucleic Acids Res* **48**: D579–D589.

Vanparys, B., Spieck, E., Heylen, K., Wittebolle, L., Geets, J., Boon, N., and De Vos, P. (2007) The phylogeny of the genus *Nitrobacter* based on comparative rep-PCR, 16S rRNA and nitrite oxidoreductase gene sequence analysis. *Syst Appl Microbiol* **30**: 297–308.

Vaser, R., Sović, I., Nagarajan, N., and Šikić, M. (2017) Fast and accurate de novo genome assembly from long uncorrected reads. *Genome Res* **27**: 737–746.

Vekeman, B., Hoefman, S., De Vos, P., Spieck, E., and Heylen, K. (2013) A generally applicable cryopreservation method for nitrite-oxidizing bacteria. *Syst Appl Microbiol* **36**: 579–584.

Vieira, A., Galinha, C.F., Oehmen, A., and Carvalho, G. (2019) The link between nitrous oxide emissions, microbial community profile and function from three full-scale WWTPs. *Sci Total Environ* **651**: 2460–2472.

Watson, M.L. (1958) Staining of tissue sections for electron microscopy with heavy metals. *J Biophys Biochem Cytol* **4**: 475–478.

Watson, S.W., and Waterbury, J.B. (1971) Characteristics of two marine nitrite oxidizing bacteria, *Nitrospina gracilis* nov. gen. nov. sp. and *Nitrococcus mobilis* nov. gen. nov. sp. *Arch Microbiol* **77**: 203–230.

Wegen, S., Nowka, B., and Spieck, E. (2019) Low temperature and neutral pH define "*Candidatus* Nitrotoga sp." as a competitive nitrite oxidizer in coculture with *Nitrospira defluvii*. *Appl Environ Microbiol* **85**: e02569-18.

Wetterich, S., Kuzmina, S., Andreev, A.A., Kienast, F., Meyer, H., Schirrmeister, L., *et al*. (2008) Palaeoenvironmental dynamics inferred from late quaternary permafrost deposits on Kurungnakh Island, Lena Delta, Northeast Siberia, Russia. *Q Sci Rev* **27**: 1523–1540.

Xia, Y., Lü, C., Hou, N., Xin, Y., Liu, J., Liu, H., and Xun, L. (2017) Sulfide production and oxidation by heterotrophic bacteria under aerobic conditions. *ISME J* **11**: 2754–2766.

Yu, X., Jiang, J., Liang, C., Zhang, X., Wang, J., Shen, D., and Feng, Y. (2016) Indole affects the formation of multicellular aggregate structures in Pantoea agglomerans YS19. *J Gen Appl Microbiol* **62**: 31–37.

Zheng, M., Li, S., Ni, G., Xia, J., Hu, S., Yuan, Z., *et al*. (2020) Critical factors facilitating *Candidatus* Nitrotoga to be prevalent nitrite-oxidizing bacteria in activated sludge. *Environ Sci Technol* **54**: 15414–15423.

Supporting Information

Additional Supporting Information may be found in the online version of this article at the publisher's web-site:

Appendix S1: Supplementary information.

Table S1. Results of qualitative monitoring of nitrite consumption of *Nitrotoga*.

Table S2. Metagenome summary.

Table S3. General genomic characteristics.

Table S4. Average nucleotide identities of *Nitrotoga* genomes.

Table S5. Information about publicly available *Nitrotoga* genomes used in this study.

Table S6. Summary of pangenome analysis.

Table S7. Summary of curated annotation.